HHS Public Access

Author manuscript

Mol Microbiol. Author manuscript; available in PMC 2016 October 01.

Published in final edited form as:

Mol Microbiol. 2015 October ; 98(3): 586–604. doi:10.1111/mmi.13144.

Mycobacterium tuberculosis oriC sequestration by MtrA response regulator

Gorla Purushotham[1], **Krishna B. Sarva**[1], **Ewelina Blaszczyk**[1,#], **Malini Rajagopalan**[1,*], and **Murty V. Madiraju**[1,*]

[1]Biomedical Research, The University of Health Science Center at Tyler, Tyler, TX-75708

Summary

The regulators of *Mycobacterium tuberculosis* DNA replication are largely unknown. Here, we demonstrate that in synchronously replicating *M. tuberculosis*, MtrA access to origin of replication (*ori*C) is enriched in the post-replication (D) period. The increased *ori*C binding results from elevated MtrA phosphorylation (MtrA~P) as evidenced by reduced expression of *dnaN*, *dnaA* and increased expression of select cell division targets. Overproduction of gain-of-function $MtrA_{Y102C}$ advanced the MtrA *oriC* access to the C period, reduced *dnaA* and *dnaN* expression, interfered with replication synchrony and compromised cell division. Overproduction of wild-type (MtrA+) or phosphorylation-defective $MtrA_{D56N}$ did not promote *ori*C access in the C period, nor affected cell cycle progression. MtrA interacts with DnaA signaling a possibility that DnaA helps load MtrA on *oriC*. Therefore, *oriC* sequestration by MtrA~P in the D period may normally serve to prevent untimely initiations and that DnaA-MtrA interactions may facilitate regulated *oriC* replication. Finally, despite the near sequence identity of MtrA in *M. smegmatis* and *M. tuberculosis*, the *M. smegmatis oriC* is not MtrA-target. We conclude that *M. tuberculosis oriC* has evolved to be regulated by MtrA and that cell cycle progression in this organisms are governed, at least in part, by oscillations in the MtrA~P levels.

Keywords

Mycobacterium; Cell cycle; Tuberculosis; Response Regulator; Synchronous replication

Introduction

Mediation of DNA replication at the origin of replication (*oriC*) by the DnaA initiator protein is an essential aspect of the cell duplication process in eubacteria and is followed by DNA segregation and cell division, the latter of which includes the FtsZ-catalyzed septal-ring assembly, septum synthesis, and cell separation steps. Much of our understanding of the regulation of the chromosomal DNA replication process comes from Gram-positive (*Bacillus subtilis*) and Gram-negative (*Escherichia coli, Caulobacter cresentus*) model organisms. However, the regulatory mechanisms operated in these bacteria are not

[*]**Address for correspondence:**Murty.Madiraju@uthct.edu, Malini.Rajagopalan@uthct.edu, Ph. 903-877-2877.
[#]Current Address: Institute of Medical Biology, Polish Academy of Sciences, 106, Lodowa St, 93-231-Lodz, Poland

All authors declare ‘no potential conflict of interest’.

necessarily similar (reviewed in (Skarstad & Katayama, 2013)). For example, *E. coli* and *B. subtilis* exhibit multi-fork replication, i. e, grow with overlapping replication cycles in nutrient-rich media, whereas *C. cresentus*, which shows a dimorphic lifestyle, does not exhibit multi-fork replication. *E. coli* uses several regulatory mechanisms that control either the availability of *ori*C or the levels and activities of DnaA for ensuring one replication event per cell cycle. These include the following: the sequestration of *ori*C by the negative regulator SeqA, the regulatory inactivation of DnaA (RIDA) by the combined action of Hda and the DNA polymerase subunit DnaN clamp, the quenching of active pools of DnaA by *datA* sequence enriched with DnaA boxes, the stimulation of DnaA-ATP hydrolysis at *datA* locus in a manner dependent upon the activity of integration-host factor, and the regulation of *dna*A transcription [reviewed in (Skarstad & Katayama, 2013)]. *B. subtilis*, does not have SeqA system, but uses the DnaA-interacting proteins Soj, SirA, and YabA for modulating DnaA activity (Murray & Errington, 2008, Noirot-Gros *et al.*, 2006, Wagner *et al.*, 2009) and the transcriptional regulator and *ori*C-binding protein Spo0A for inhibiting initiation of DNA replication at the onset of sporulation (Castilla-Llorente *et al.*, 2006). *C. cresentus* uses response regulator (RR) CtrA-dependent cascade type of regulation to sequester *oriC*. CtrA-mediated regulation is, however, dependent on its proteolytic stability and phosphorylation status (Domian *et al.*, 1997, Quon *et al.*, 1998). Interestingly, *C. cresentus* DnaA levels, unlike its counterparts, are unstable and oscillate as a function of the cell cycle, thus contributing to the regulation of replication (Gorbatyuk & Marczynski, 2005). Finally, other RR such as ArcA in *E. coli* and HP1021 in *Helicobacter pylori* have also been reported to interact with *oriC* and interfere with the replication initiation process in vitro (Donczew *et al.*, 2015, Lee *et al.*, 2001).

It is unknown how the DNA replication process in *Mycobacterium tuberculosis*, the causative agent of tuberculosis (TB), is regulated. *M. tuberculosis* is a slow-grower with an average doubling time of 24 hours (h). TB accounts for nearly 1. 5 million deaths per year and one-third of the global population are latently infected with *M. tuberculosis*. It is known that *M. tuberculosis* successfully shifts between active and clinically asymptomatic latent (persistent) growth states in response to immune pressure (Smith, 2003). Although the doubling times of latent *M. tuberculosis* in humans cannot be assessed and are expected to be high, immune-restrained *M. tuberculosis* replicate during persistent growth in mice lungs (Gill *et al.*, 2009). Intuition is that the replication and cell cycle processes must be tightly controlled during latency and reactivation. Published data showed that the *M. tuberculosis dnaA-dnaN* intergenic region serves as *oriC* (Qin *et al.*, 1999), and *M. tuberculosis* DnaA ATP-hydrolysis activity is required for its rapid oligomerization on *oriC*, a result different from that seen in *E. coli*. Additionally, DnaA defective for ATP-hydrolysis is non-functional in vivo (Madiraju *et al.*, 2006) and synchronously replicating *M. tuberculosis* do not show hyper-initiation (Nair *et al.*, 2009). Finally, Rv1985c gene product has been shown to bind *M. tuberculosis oriC* at the AT-rich region in vitro and prevent *ori*C duplex unwinding when added prior to the addition of DnaA (Kumar *et al.*, 2009), however, the biological significance of these findings have not been evaluated. Recent cell cycle studies with *M. smegmatis*, a rapid grower with a doubling time of 3 h and a nonpathogen, indicate that *M. smegmatis* does not exhibit multi-fork replication (Santi *et al.*, 2013, Trojanowski *et al.*,

2015) and that their cell cycle organization is distinct compared with well-known model organisms (Santi et al., 2013).

MtrA is the essential RR component of the MtrAB histidine-aspartate two-component response regulatory system (2CRS) of *M. tuberculosis* (Zahrt & Deretic, 2000). Earlier studies showed that MtrA is poorly phosphorylated in vitro (Friedland *et al.*, 2007, Rajagopalan *et al.*, 2010); D56 residue is important for MtrA phosphorylation and replacement of D with N residue abolished MtrA phosphorylation ability (Fol *et al.*, 2006); phosphorylated MtrA (MtrA~P) binds *oriC* in vitro at four different locations, designated as MtrA-boxes F2, F3, F4 and F5 (Rajagopalan et al., 2010). The arrangement of the MtrA- and DnaA- boxes on *oriC* is non-overlapping (Rajagopalan et al., 2010). It is shown that promoters (*P*) for *dnaA*, secreted antigen 85B and cell wall mycolyl transferase (*fbpB*), and essential cell wall hydrolase, *ripA* are MtrA-targets (Fol et al., 2006, Plocinska *et al.*, 2012, Rajagopalan et al., 2010). Other studies showed that *M. tuberculosis* multiplication upon infection depends, in part, on the optimal ratios of phosphorylated to nonphosphorylated MtrA (Fol et al., 2006). While these data connect MtrA levels/phosphorylation activity to cell cycle (i.e. replication and cell division) and possibly other processes, the biological significance of MtrA binding to *oriC* and the roles of MtrA~P, if any, on *oriC* replication are unknown. The present study was undertaken to evaluate the roles of MtrA in *M. tuberculosis* DNA replication. Characterization of the MtrA-*oriC* interactions under synchronous replication conditions led us to conclude that MtrA~P functions as a regulator of *ori*C replication. These studies also showed that MtrA interacts with DnaA and that *M. smegmatis oriC* is not MtrA target. Our studies suggest that the *M. tuberculosis oriC* has evolved to be regulated by MtrA and that the MtrA-mediated regulation of DNA replication is different from that known in other organisms.

Results

MtrA~P binds preferentially to *oriC*

Two series of experiments were performed to evaluate MtrA~P binding to *oriC* (Fig. 1 A). First, MtrA or MtrA~P binding to full-length *oriC* was detected by electrophoretic gel-mobility shift assay (EMSA). MtrA~P was produced by incubating MtrA with *E. coli* EnvZ kinase and ATP or ^{32}P-ATP as described (Fol et al., 2006). Incubation of MtrA with EnvZ led to a time dependent increase in MtrA phosphorylation (Fig. 1 B). EMSA experiments clearly showed that MtrA~P bound *oriC* better than MtrA (Fig. 1 C-i, ii). Following densitometry, the fraction of free *oriC* was calculated, the total bound *oriC* was determined and a plot of the percent bound *oriC* versus in put MtrA concentration was prepared (Fig. 1 C-iii). It should be noted that the fraction of bound *oriC* includes both stable and unstable MtrA~P-*oriC* complexes in the reaction. These data revealed a sigmoidal curve typical of cooperative binding (affinity of MtrA~P to *ori*C increases upon binding of some MtrA~P), with a Hill coefficient of 3.2 (± 0.22), and apparent dissociation constant K_D of 410 nM (± 0.014). The *oriC* fragment contains 4 MtrA-binding sites (Fig. 1 A) and a perfect cooperative binding is expected to give a Hill coefficient of 4. Thus, the measured 3. 2 Hill coefficient number is indicative of highly cooperative system where all MtrA binding sites in *oriC* are occupied interdependently by MtrA~P. The measured K_D could be a large

overestimate as it was based on the assumption that the recombinant MtrA is fully active and is efficiently phosphorylated.

On the other hand, nonphosphorylated MtrA showed inefficient binding and MtrA-*oriC* complexes were relatively unstable (Fig. 1 C, compare ii with i). The MtrA-*oriC* complexes were detected at relatively high protein concentrations, i.e. 1.60 μM (lane 9) with apparent K_D of 1.7 μM (± 0.008). The observed poor binding of MtrA to *oriC* is consistent with our published footprinting data (Rajagopalan et al., 2010). Similar binding pattern was also noted for other targets (see below). EMSA studies with DNA-fragments bearing individual MtrA-boxes revealed modest MtrA~P binding to the F2 box (Fig. 1 C-iv) and that the binding was abolished when the F2 box was replaced with a mutant sequence demonstrating the specificity of MtrA-*ori*C interactions (Fig. 1 C-v, see EMSA methodology section for mutant F2 box sequence). No detectable MtrA binding to *oriC* DNA fragments containing the individual F3, F4 or F5 boxes was detected (data not shown). Presumably, F2 box with GTCACA sequence is the preferred motif and is likely accessed first by MtrA~P in vivo followed by other MtrA-boxes. It should be noted that the F2 MtrA-box is located between the AT-rich DNA unwinding element (DUE) and a DnaA-box (Fig. 1 A) and is conserved in diverse *Mycobacterium spp.* Also, the loss of the GTCACA motif abolished autonomous replication activity of *oriC* plasmids (Rajagopalan et al., 2010). Further studies with more sensitive assays are required for evaluating the kinetics, order and consequences of MtrA-binding to *oriC* MtrA-boxes in the presence and absence of DnaA.

Next, we performed solid-phase binding experiments wherein biotinylated *oriC* coupled to streptavidin magnetic beads was incubated with varying concentrations of MtrA or MtrA~P, magnetically separated, resolved by SDS-PAGE, immunoblotted and band signal intensities corresponding to MtrA quantitated by densitometry (Fig. 1 D-i a). Again, distinct differences between MtrA and MtrA~P processed samples were noted. For example, bands corresponding to MtrA~P were detected at lower protein concentrations as compared to MtrA (compare lanes 3–7 with 9–13). The calculated ratio of bound MtrA~P to MtrA revealed a five-fold difference in signal intensity (Fig. 1 D-i b). MtrA or MtrA~P did not bind *PftsZ* under these conditions indicating that *oriC* is a specific target (Fig. 1 E). Finally, consistent with the EMSA data, MtrA~P bound to DNA fragment bearing F2 WT sequence, but not to that containing mutant sequence (Fig. 1 D-ii, iii). Together, these data emphasize that MtrA~P binds better than MtrA to *oriC* and F2 box.

$MtrA_{Y102C}$ binds *oriC* and DNA fragments bearing individual MtrA-boxes

MtrA crystal structure data revealed that the amino-terminal regulatory and carboxy-terminal effector domains are oriented in such a way that extensive contacts between these two lock the regulatory domain in inactive conformation leading to decreased activation (Friedland et al., 2007). This could in turn lead to inefficient target binding. These data also revealed that Y102 residue is oriented away at outward position and hydrogen bonded with D190 of the DNA-binding domain, thereby bridging the stability of domains (Friedland et al., 2007). In an effort to identify MtrA proteins exhibiting enhanced phosphorylation activities, we characterized several MtrA mutant proteins and found that $MtrA_{Y102C}$ is phosphorylation-competent (Al Zayer *et al.*, 2011, Plocinska et al., 2012), acts as a gain-of-

function (GoF) protein that functions in the absence of MtrB (Plocinska et al., 2012). We then investigated $MtrA_{Y102C}$ interaction with *oriC*. In vitro phosphorylation experiments revealed that $MtrA_{Y102C}$ exhibits higher rates and yields of phosphorylation as compared to MtrA (Fig. 1 B). EMSA studies showed that $MtrA_{Y102C}$ bound *oriC* with and without phosphorylation similarly with apparent of K_D of 0.23 μM (± 0.002) (Fig. 2 A- i–iii). $MtrA_{Y102C}$ bound DNA fragments bearing F2 (Fig. 2 A–iv) but not mutant box (Fig. 2 A-v); also unlike the situation with MtrA~P, it bound F3, F4 and F5 boxes (Fig. 2 B i–iii). Data from solid phase DNA binding experiments were also consistent with EMSA data (Fig. 2 C-i–iii). Altered DNA binding properties of $MtrA_{Y102C}$ are likely due to Y102C change that destabilizes the MtrA inter-domain orientation thereby promoting active conformation of the regulatory domain. A consequence could be enhanced rate of phosphorylation (Fig. 1 B) and target binding (Fig. 2). The ability of $MtrA_{Y102C}$ to bind DNA fragments bearing individual MtrA-boxes further supports the notion that MtrA phosphorylation promotes *oriC* binding and that MtrA-boxes in *oriC* are occupied under optimal MtrA~P conditions.

MtrA binding to *oriC* is associated with modulation of *dna*N transcription

dnaN is located downstream of *oriC* (Fig. 1 A). The nucleotide sequences of *oriC* and *dnaN* of *M. tuberculosis* and the closely related vaccine strain *M. bovis* BCG are nearly identical; also *M. tuberculosis oriC* is functional in *M. bovis* BCG (Qin et al., 1999, Salazar *et al.*, 1996). Primer extension studies identified *M. bovis* BCG *dnaN* promoter in the *oriC* 3' end with two transcription start sites designated as T1 and T2 at nucleotides −110 and −258 relative to *dnaN* start codon (Salazar *et al.*, 2003). Although *M. tuberculosis PdnaN* is not determined, given the conserved organization of *ori*C and flanking regions of *M. tuberculosis* and *M. bovis* BCG, we assumed that *M. tuberculosis PdnaN* is located in its *ori*C (see Fig. 1 A '*' above G residues for presumptive T1 and T2 sites). Accordingly, we considered a possibility that one consequence of MtrA binding to *oriC* is the modulation of *dnaN* transcription. Hence, we evaluated *dnaN* transcription by qRT-PCR relative to 16S rRNA under steady-state growth conditions in *M. tuberculosis* strains producing either normal (control) or elevated levels of wild-type (WT) MtrA (MtrA+; Rv78), $MtrA_{Y102C}$ (RvY102C) or phosphorylation-defective $MtrA_{D56N}$ (Rv129, (Fol et al., 2006), see Table S2 for strains and plasmids) and the data were normalized relative to control. The *dnaN* transcription showed a significant reduction in RvY102C, but was modestly decreased in Rv78 and elevated in Rv129 (Fig. S1). Earlier studies revealed that $MtrA_{D56N}$ does not bind DNA fragment bearing MtrA-boxes (Al Zayer et al., 2011). The F3 MtrA- box and one of the promoters of *dnaN* overlap (see Fig. 1A). Perhaps, the compromised affinity of $MtrA_{D56N}$ towards the F3 MtrA-box in the Rv129 background resulted in increased *dnaN* transcription. Nonetheless, these data support a notion that $MtrA_{Y102C}$ overproduction leading to aberrant MtrA~P is associated with reduction in *dnaN* transcription.

MtrA accesses *oriC* after the DNA synthesis period of cell cycle

To determine the biological consequences of MtrA interactions with *oriC*, we first sought to determine the specific timing of their interactions during the cell cycle process. To this end, we used synchronously replicating cultures for evaluating DNA replication and for determining the MtrA-occupancy of *oriC* by ChIP (see below). We recently engineered and characterized three *dnaA* cold-sensitive (*Mtb dna*Acos) strains (Nair et al., 2009) and

evaluated their ability to show synchronous replication following the earlier published protocols (Dick *et al.*, 1998, Lim *et al.*, 1999, Wayne, 1977). These studies revealed that the engineered *Mtb dna*Acos strains are cold-sensitive for replication initiation at nonpermissive (30°C) temperature, but resume synchronous replication after a lag of 2 to 4 h upon shift to a permissive (37°C) temperature (Nair et al., 2009). One of the strains, *Mtb dna*Acos115, referred to as *dna*Acos hereafter, was characterized further. Consistent with the published report (Nair et al., 2009), we observed synchronous replication following temperature shift from 30°C to 37°C and found that the typical DNA synthesis period (a round of replication leading to the doubling of the initial counts) lasted for 12 h, whereas the inter-replication period was approximately 10 to 12 h (Fig. 3 A). For clarity, DNA synthesis period was defined as the C period and the time interval between two replication cycles as the D period (see Fig. 3 A). The C period includes the initiation (i.e. the initial interactions between DnaA and *ori*C leading to the formation of the initiation complex) and the DNA chain-elongation steps. Thus, the D period in this study is different than the traditional one defined for *E. coli* cell cycle, which is the time between the end of chromosome replication and cell division (Cooper & Helmstetter, 1968). DNA incorporation studies revealed a 2 h lag (pre-replication period) in the first cycle of replication, which is presumably due to a slow build up of DnaA and possibly other cofactors necessary for the assembly of *M. tuberculosis* orisome. CFU analysis revealed the doubling of the cell number by 30 h (Fig. S 2). It is unknown if DNA segregation is initiated and completed within the D period and/or overlaps with the C period of second cycle, but it is likely that cell division initiated in the first cycle is completed during the second cycle of replication. These latter results are similar to the situation reported with *M. smegmatis* single-cell-dynamics studies (Santi et al., 2013).

MtrA ChIP-PCR for *ori*C followed by normalization to the control target, *PftsZ* (Rajagopalan et al., 2010), revealed significant (i.e., normalized ratio of 2 and above with p-values below <0.05) *oriC* enrichment at 18 and 24 h (i.e., in cells with no ongoing DNA replication) and again after 42 and 48 h, but none in the C period (Fig. 3 B). ChIP-PCR experiments with DnaA-antibodies revealed, as expected, the DnaA enrichment of *oriC* in the C period with detectable binding in the D period (Fig. 3 C, see 12 and 18 h).

oriC sequestration in the D period by MtrA is not due to changes in the *mtrA* transcript and protein levels

Several experiments were carried out to understand why MtrA occupancy of *oriC* was enriched in the D period. First, we measured the *mtrA* transcript levels by qRT-PCR in *dna*Acos at various periods after initiation of synchronous replication, normalized to 16S rRNA and determined fold expression relative to time ‘0’ (Fig. 4 A). As can be seen, *mtrA* transcription was reduced at non-permissive temperature, i.e. 30°C (Fig. 4 A- ii), but steadily increased up to 6 h and remained fairly high thereafter (Fig. 4 A). These results suggest that *mtrA* transcription is high in actively replicating cells. As a control, we measured *dosR* RR expression and found that it remained low in both C and D periods (Fig. S 3). Next, we evaluated by immunoblotting the intracellular MtrA levels relative to the house-keeping SigA protein (Fig. 4 B-i). Consistent with the *mtrA* transcription profiles, MtrA protein levels were low at 30°C compared to 37°C (Fig. 4 B – ii, iii), gradually increased up to 12 h, thereafter were high and remained fairly constant (Fig. 4 B -i). We

conclude from these data that *ori*C enrichment by MtrA in the D period is not due to changes in the *mtrA* transcript and protein levels.

Next, we considered whether increased *oriC* enrichment in the D period is in part due to increased MtrA phosphorylation. To address this issue, we aimed to measure MtrA~P in both C and D periods by two independent measures. First, we attempted to detect and distinguish the MtrA and MtrA~P forms using Phos-tag acrylamide gels among other methods, but met with limited success. Because a consequence of RR phosphorylation is the modulation of target gene expression, as an alternative measure for MtrA~P status, we evaluated the expression levels of MtrA-targets, *dnaN* (see above Fig. S 1), *dnaA* (Fol et al., 2006), *ripA* (Plocinska et al., 2012) and others (identified based on our MtrA ChIP-Seq studies; see below), during synchronous replication. The *dnaN* transcription, relative to 16S rRNA, showed a sharp increase between 6 and 12 h followed by return to basal levels and decreased thereafter. Another burst of *dnaN* transcription occurred between 30 to 42 h and decreased thereafter (Fig. 4 C-i). A similar trend was also noted with the *dnaA* expression (Fig. 4 C-i). Thus, the periodic *dnaN* and *dnaA* expression show inverse correlation with the MtrA-occupancy of *ori*C. Like *oriC*, the immediate 5' upstream region of *dnaA* contains MtrA binding sites [(Li *et al.*, 2010), see also Fig. S 4A]. ChIP-PCR studies with MtrA antibodies revealed *PdnaA* enrichment in both C and D periods, with modestly elevated levels at 12 and 18 h (Fig. S 4B) indicating that MtrA binds *PdnaA*. We infer from these data that increased expression levels of *dnaA* and *dnaN* are required during the C period and that MtrA~P likely functions as a transcriptional repressor of *dnaA* and *dnaN*.

The above data lead to a hypothesis that MtrA activity, hence MtrA~P, is temporal. To validate this hypothesis, we evaluated the expression profiles of select MtrA-targets involved in other aspects of cell cycle, i.e. cell division. We recently performed MtrA ChIP-Seq in *M. tuberculosis* producing $MtrA_{Y102C}$ background, elucidated the comprehensive MtrA-regulon (Madiraju and Rajagopalan, unpublished data), and selected *dacB*1, *sepF, pbpB, ripA, rpfB, whiB*2 and *clpX* as potential MtrA-targets for this study. In addition, expression profiles of non-targets *murD* and *mtrB* were measured. The nucleotide sequences upstream of the selected targets contained distinct MtrA-binding motifs (Table S3). EMSA with select target genes confirmed MtrA~P binding to their upstream regions (Fig. S 5, note inefficient binding of MtrA to these targets). QRT—PCR data revealed that although *ftsI, dacB1* and *sepF* were expressed in both C and D periods, their expression was elevated in the D period (Fig. 4 C-ii); other targets, i.e. *rpfB, ripA, clpX* and *whiB2* did not show such changes (Fig. 4 C-iii). We conclude that expression of not all MtrA-targets is temporal and that MtrA~P pools, although maintained in both the C and D periods, are elevated in the D period.

DnaA protein acts as a transcriptional regulator and since the *dna*A transcript levels were reduced in the D period (Fig. 4 C-i), the possibility that decreased *dna*A expression in the D period contributes to increased *ftsI, dacB1, and sepF* expression remains open. This possibility implies that DnaA acts as a transcriptional repressor of the above genes. To address this concern, expression levels of these targets in *M. tuberculosis* overexpressing *dnaA* were measured. Little or no changes to the expression levels of *mtrA, ftsI, dacB1* and *sepF* and a modest 2.5 fold reduction of *whiB2* was observed (Fig. S 6), thus alleviating the

concern that the observed changes in the MtrA-target expression are due to changes in the *dnaA* expression levels, but likely due to increased MtrA activity.

Untimely MtrA~P access to *oriC* interferes with *oriC* replication

Next, we evaluated the consequences associated with the untimely MtrA~P access to *oriC* in the C period. Towards this end, we wished to create a *M. tuberculosis* strain producing the GoF $MtrA_{Y102C}$ as the sole source for MtrA in the *dna*Acos background by recombineering approach ((van Kessel & Hatfull, 2008), but met with limited success (not shown); presumably, unregulated MtrA~P owing to $MtrA_{Y102C}$ production is toxic to *M. tuberculosis* growth and viability. As an alternative, we created and characterized a *dna*Acos meropdiploid expressing *mtrA* from the tetracycline-inducible promoter (Ehrt *et al.*, 2005). Addition of anhydrotetracycline (*atc*) at the time of initiation of synchronous replication led to elevated *mtrA* transcript and protein levels in both the C and D periods (Fig. S 7 A/B). The DNA synthesis pattern was, however, different from that seen with the *dna*Acos (Fig. 5 A). A steady increase in DNA synthesis up to 30 h corresponding to nearly three rounds of DNA replication was noted; no additional increase in DNA synthesis beyond 30 h was observed (Fig. 5 A- compare with Fig. 3 A). Also, no lag or pre-replication period was detected under these conditions. The distinct inter-replication period, as seen with the *dna*Acos, was absent (compare Fig. 5 A with 3A). These data suggest that elevated $MtrA_{Y102C}$ allows untimely initiations. CFU analysis showed cell doubling by 30 h (Fig. S 8 -A).

ChIP-PCR analysis with MtrA antibodies revealed significant *oriC* enrichment from 12 h onwards, but detectable *oriC* enrichment (IP:Mock ratios 2 and high) also occurred at 2 and 6 h (Fig. 5 B) indicating that $MtrA_{Y102C}$ accessed *oriC*, albeit modestly, in the C period and affected replication synchrony. These results indicate that DNA synthesis under $MtrA_{Y102C}$ overproduction conditions is asynchronous and leads to eventual DNA synthesis arrest. *OriC*-DnaA ChIP experiments revealed that DnaA accessed *oriC* at all time periods, but increased access resulting in elevated enrichment was noted from 12 h onwards (Fig. 5 C compare with Fig. 3 C). These results are similar to those for $MtrA_{Y102C}$ occupancy of *oriC* (Fig. 5 B). Perhaps, MtrA and DnaA interact (see below) and such interactions impact their associations with *oriC* (see below).

To examine whether the observed effects are specific to $MtrA_{Y102C}$, we overexpressed in the *dna*Acos background either WT *mtr*A (*dna*Acos/MtrA+) or phosphorylation-defective *mtr*A (*dna*Acos/$MtrA_{D56N}$). Addition of *atc* increased their expression levels to similar extents (Fig. S 9 A/B). The DNA synthesis profiles, however, revealed differences between the two. For example, the *dna*Acos/MtrA+ showed the completion of two replication cycles by 12 h followed by a distinct D period and another burst of replication after 24 h (Fig. 6 A, see incorporation levels). Pre-replication or lag period, as observed for *dna*Acos (Fig. 3 A) was not observed. Interestingly, the DNA synthesis pattern of the *dna*Acos/$MtrA_{D56N}$ was similar to *dna*Acos (Fig. 6 B). Together, these data indicate that MtrA overproduction can promote DNA synthesis in the C period provided that MtrA is competent for phosphorylation. Next, we examined the MtrA-occupancy of *oriC*. Similar to *dnaAcos*, maximal *oriC*-enrichment by MtrA was noted at 12, 18 and 24 h with both *dna*Acos/MtrA+

and *dna*Acos/MtrA$_{D56N}$ (Fig. 6 C and D, compare with Fig. 3 B). Despite stimulation of DNA synthesis upon MtrA overproduction (*dna*Acos/MtrA+), significant *oriC* enrichment was not observed in the C period emphasizing that MtrA access to *oriC* is regulated. DnaA-occupancy of *oriC* in the *dna*Acos/MtrA+ revealed *oriC* enrichment in both C and D periods with increased levels in the D period (Fig. 6 E). The *dna*Acos/MtrA$_{D56N}$ DnaA-occupancy of *oriC* data were similar to that seen with *dna*Acos (Fig. 6 F). CFU analysis revealed cell doubling by 30 h in both cases (Fig. S 8 -B and C). We infer from these data that overproduction of GoF MtrA$_{Y102C}$, which likely leads to elevated MtrA~P pools, promotes *oriC* access in the C period and promotes untimely initiations.

Aberrant MtrA~P impacts the MtrA-target expression

Next, we evaluated the MtrA-target expression in the *dna*Acos/MtrA$_{Y102C}$ during synchronous replication essentially as described for Fig. 4. The *dnaA* and *dnaN* expression levels were high till 12 h, but reduced significantly at 18 h and beyond (Fig. 7 A and compare with Fig. 4 C-i). While the reduced *dnaA* and *dnaN* expression levels correlate well with the blocked DNA synthesis, their expressions levels remained high till 12 h. Both *oriC* and *PdnaA* contain DnaA- and MtrA- boxes [see Fig. 1 A, S 4, (Fol et al., 2006, Li et al., 2010, Rajagopalan et al., 2010)]. Perhaps, MtrA ability to access these targets is governed by other proteins, e.g. DnaA, thereby delaying the MtrA~P-mediated transcriptional repression. We also found that the *ftsI*, *dacB1*, *sepF* and *whiB2* expression in the *dna*Acos/MtrA$_{Y102C}$ was aberrant (Fig. 7 B, compare with Fig. 4 C-ii, note that *sep*F expression pattern was different indicating a complex regulation of its expression). Thus, elevated MtrA~P overproduction leads to aberrant target expression.

Production of GoF MtrA$_{Y102C}$ is associated with altered shape and induction of the SOS response

The cell morphology of *dnaAcos* and *dna*Acos/MtrA$_{Y102C}$ were similar at 0 h (see Fig. 7 C panels i/ii vs iii/iv). However, the *dna*Acos/MtrA$_{Y102C}$ cells at 48 h were elongated when compared to *dnaAcos* (Fig. 7 C, compare panel vii with v). Nucleoid staining by propidium iodide revealed that elongated cells contained unresolved nucleoids (Fig. 7 C, compare panel viii with vi). The cell morphology of *dna*Acos/MtrA+ and *dna*Acos/MtrA$_{D56N}$ was similar to that noted with the *dna*Acos (data not shown). Blocked DNA synthesis leading to altered cell shape also implies stress and possible induction of the SOS response. The LexA-regulon and induction of the SOS response in *M. tuberculosis* have been well investigated (Rand *et al.*, 2003, Smollett *et al.*, 2012). Evaluation of the expression of select targets involved in the SOS response which are under LexA-RecA control, e.g. *recA*, *lexA*, *ruvC*, *dnaE2*, *chiZ* and LexA-dependent, but RecA-independent, e.g. Rv1057, in *dna*Acos/MtrA$_{Y102C}$ relative to *dna*Acos revealed their upregulation at 18 and 48 h (Fig. 7 D). In contrast, *fts*Z, which is not a member of the LexA-regulon, was not significant changed. Together, these results support the notion that the *dna*Acos/MtrA$_{Y102C}$ cells are stressed.

MtrA interacts with DnaA

Given the effects of MtrA~P on *ori*C replication and regulation of *dna*A transcription, we considered a possibility that MtrA interacts with DnaA. Consistent with this prediction, *E.*

coli based bacterial-2-hybrid assays revealed pair-wise interactions between MtrA-DnaA and DnaA-DnaA, similar to the positive control GCN4-GCN4. The β-galactosidase activities of the DnaA-DnaA and MtrA-DnaA pairs were comparable to the positive control (Fig. 8 A). We also found interactions between $MtrA_{D56N}$ and DnaA (not shown). To further validate these interactions in mycobacterial host, we performed pull-down assays with recombinant *M. smegmatis* producing *M. tuberculosis* DnaA-His protein (see methodology for details). *M. smegmatis* lysate carrying DnaA-His was mixed with that overproducing MtrA, allowed to bind Ni-NTA resin, washed, the bound proteins were eluted and immunoblotted with DnaA and MtrA antibodies for detecting DnaA and MtrA, respectively. The fractions containing DnaA also contained MtrA indicating interactions between these two proteins (Fig. 8 B, panels i and ii). Controls showed that MtrA *per se* did not bind to the Ni-NTA resin (Fig. 8 B, panel iii). Together, these data confirm interactions between MtrA and DnaA.

MtrA does not bind *M. smegmatis oriC*

We reported earlier that among the four *ori*C MtrA-boxes, only the F2-box is conserved in *M. smegmatis* (Rajagopalan et al., 2010). This, combined with the near sequence identity of MtrA proteins and the conserved *mtr*AB regions, raises a question as to whether the *M. smegmatis ori*C is MtrA target and if so, whether the MtrA-mediated effects on *ori*C replication in *M. smegmatis* are similar to *M. tuberculosis*. The *M. smegmatis* counterpart of *M. tuberculosis dnaAcos* is not available. Nonetheless, to evaluate MtrA role in *oriC* replication, a series of experiments were carried out. First, we determined the *M. smegmatis oriC* plasmid transformation frequency, a measure for *ori*C plasmid replication. We found that *M. smegmatis oriC* plasmids with WT (Qin *et al.*, 1997)) or mutant F2 box sequences (pEBM9, see Table S2) showed a similar transformation efficiency (~0.3×10^3 transformants/μg DNA). The respective *oriC* plasmids were also recovered from these transformants (data not shown). These results stand in stark contrast to the situation reported with *M. tuberculosis oriC* plasmids because *oriC* plasmids with mutations in the MtrA-boxes could neither be transformed nor recovered (Rajagopalan et al., 2010).

Second, we performed *oriC* ChIP-PCR experiments using MtrA antibodies with lysates prepared from *M. smegmatis* producing either normal (data not shown) or elevated MtrA levels and normalized data to *Pfts*Z (Fig. 9 A). No *ori*C enrichment was detected (see Fig. 9 A). MtrA antibodies, however, enriched the MtrA-target promoters *PfbpB* (Fig. 9 A) and *PripA* (not shown, see (Plocinska et al., 2012)) under the same conditions indicating that the failure to enrich *ori*C is not due to technical limitations. *OriC* enrichment also did not occur with *M. smegmatis* containing extra copies of *M. smegmatis oriC* on a plasmid [Fig. 9 B, (Qin et al., 1999, Qin et al., 1997)], but significant *ori*C enrichment occurred with *M. smegmatis* harboring *E. coli-Mycobacterium* shuttle vector containing *M. tuberculosis oriC* sequence (Fig. 9 B, see *oriC*-TB lane). The use of shuttle plasmids was necessary for the maintenance of *M. tuberculosis oriC* sequences in *M. smegmatis* as the *M. tuberculosis oriC* is not functional in *M. smegmatis* (Qin et al., 1999). Thus, selective enrichment of *M. tuberculosis oriC* (Fig. 9 B, see lane *ori*C-TB), *M. smegmatis PfbpB* (Fig. 9A) and *pripA* (data not shown) by ChIP with MtrA antibodies in *M. smegmatis* lysates supports the notion that *M. smegmatis oriC* is not MtrA target, whereas *M. tuberculosis ori*C is a target. Finally,

replacement of *M. smegmatis ori*C on the chromosome with *oriC* carrying mutant F2-box sequence by homologous recombination did not lead to any measurable defects in growth and viability under the experimental conditions investigated here (data not shown). Taken together, these results suggest that MtrA does bind *M. smegmatis ori*C.

Discussion

Although the whole genome sequence of *M. tuberculosis* was published over 14 years ago (Cole *et al.*, 1998), the potential regulators of *M. tuberculosis ori*C replication have not been defined. Our studies connect the essential MtrA RR (Zahrt & Deretic, 2000) to the regulation of *ori*C replication and reveal that MtrA exerts regulatory effects on *ori*C DNA replication (see below). Furthermore, the MtrA-mediated regulatory effects are linked to its phosphorylation state (see below).

MtrA~P: negative regulator of *ori*C replication

oriC DNA binding experiments (Figs. 1, 2) combined with our earlier published footprinting data (Rajagopalan et al., 2010) support the notion that MtrA~P binds cooperatively to its binding sites in *oriC*. We showed that in synchronously replicating cells producing normal levels of MtrA~P, MtrA sequesters *oriC* (Fig. 3), represses *dnaA* and *dnaN* transcription and promotes *ftsI*, *dacB1* and *sepF* transcription [Fig. 4 C, see also (Fol et al., 2006, Li et al., 2010)] in the D period. Our results also revealed that *mtrA* transcript and protein levels were similar in the C and D periods (Fig. 4). We infer from these data that pools of MtrA~P, hence MtrA~P to MtrA ratio, are elevated in the D period. Overproduction of GoF $MtrA_{Y102C}$ advanced MtrA~P to the C period and enabled MtrA access to *oriC* (Fig. 5 B); this untimely *oriC* access, although stimulated DNA synthesis during the initial period (see below), led to eventual DNA synthesis blockage, defects in cell division, repression of *dnaA* and *dnaN* transcription (Figs. 5 A, 7). Together, these results are consistent with a hypothesis that MtrA~P acts as a negative regulator of *oriC* replication wherein it sequesters *oriC* and represses *dnaA* and *dnaN* transcription to prevent untimely initiations in replicating cells. The concept that pools of MtrA~P are elevated in the D period is not unreasonable because phosphorylation of MtrB sensor kinase (also referred to as activation), which is necessary for MtrA~P and MtrA-target expression, is promoted upon MtrB septal association (Plocinska et al., 2012). Presumably, viable septa necessary for promoting MtrB activation are abundant during or after the replication cycle, and once activated, MtrB~P promotes MtrA~P thereby elevating the ratios of MtrA~P to MtrA. This could in turn lead to *ori*C sequestration, repression of *dna*A and *dna*N transcription, stimulation of the expression of MtrA-targets *fts*I, *sep*F, *dac*B1 critical for septum synthesis and cell division and optimal cell cycle progression; all of these events are impacted upon $MtrA_{Y102C}$ overproduction. Thus, DNA replication and cell cycle progression in *M. tuberculosis* are governed, in part by oscillations in the MtrA phosphorylation levels.

Despite DnaA association with *oriC*, reinitiation did not take place in the D period (Fig. 3 C). One reason for this could be that the DnaA oligomerization state in the C and D periods is different, hence DnaA-*oriC* complexes in the D period are not proficient at initiating new rounds of replication. One caveat to this argument is that the nucleotide-bound states of

DnaA during *M. tuberculosis* cell cycle progression are unknown. While both DnaA.ATP and DnaA.ADP forms bind *ori*C with similar affinity, only DnaA competent to bind and hydrolyze ATP is proficient for the formation of oligomeric complexes and *oriC* unwinding in vitro (Kumar et al., 2009, Madiraju et al., 2006, Yamamoto *et al.*, 2002), and possibly for replication initiation in vivo (Madiraju et al., 2006). This makes us think that at least a majority of the DnaA bound to *oriC* in the C period is the DnaA.ATP form, hence competent for replication initiation. On the other hand, the non-overlapping arrangement of DnaA and MtrA boxes, the location of DUE relative to F2 box (Fig. 1A), combined with the observed interactions between DnaA and MtrA (Fig. 8) leads to an alternate hypothesis that DnaA helps load MtrA on *oriC* in the D period, and that MtrA binding to *oriC* and DnaA limits subsequent DnaA oligomerization, organization of DnaA.ATP-initiation complex competent for replication and or *oriC* unwinding in the D period. These possibilities are not mutually exclusive.

Our results showing that elevated ratios of MtrA~P to MtrA result in the repression of *dnaA* transcription are consistent with a recent report showing that *PdnaA* activity is increased in the *lpqB* mutant background containing decreased levels of MtrA~P (Nguyen *et al.*, 2010). It is pertinent to note that *dna*A transcription is shown to be elevated in *M. tuberculosis* overexpressing MtrA+ upon infection in monocyte-derived macrophages (Fol et al., 2006). Presumably, the regulation of *dna*A transcription upon infection is rather complex, possibly involving the activities of hitherto uncharacterized regulators (Galagan *et al.*, 2013).

MtrA~P: positive regulator of *ori*C replication

Stimulation of DNA synthesis without significant *oriC* enrichment upon MtrA+ overproduction (Fig. 6 A/C, compare with panel B/D) signals a possibility that MtrA~P exerts a positive regulatory effect on *oriC* replication. Our results showing little or no pre-replication period under MtrA+ overproduction conditions (Fig. 7 A/B) and severely compromised *oriC* plasmid transformation efficiency of *oriC* MtrA-box mutant plasmids (Rajagopalan et al., 2010) are in partial agreement of a concept that MtrA promotes *oriC* replication. Overproduction of GoF $MtrA_{Y102C}$ also promoted DNA synthesis and suppressed the lag or pre-replication period (Fig. 5 A). While the precise mechanisms as to how MtrA~P exerts positive regulatory effect are unknown, it is likely that MtrA interactions with DnaA are important in this regard. One possibility is that MtrA remains associated with DnaA at the end of the D period despite its dissociation from *oriC* owing to a reduction in the MtrA~P pools, and facilitates increased DnaA oligomerization on *oriC* and the DnaA-mediated *oriC* initiation complex formation, perhaps analogous to the situation seen with DiaA protein of *E. coli* (Keyamura *et al.*, 2007) and HobA of *H. pylori* (Zawilak-Pawlik *et al.*, 2007). Another possibility is that MtrA/DnaA interactions promote the stability of DnaA, if any, thereby increase the intracellular pools of DnaA necessary for initiation. A consequence would be suppression of pre-replication period and stimulation of *oriC* replication. Nonetheless, we think that MtrA is an auxiliary factor of the *M. tuberculosis* replisome machinery in normally replicating cells, and that MtrA~P acts as a negative regulator in the D period and a positive regulator in the C period. A cartoon showing the MtrA~P mediated regulatory effects on *ori*C replication is shown (Fig. 10).

OriC sequestration and repression of *dnaA* and *dnaN* transcription in nonreplicating cells are likely the control mechanisms operating for limiting reinitiation in the D period. What then are the mechanisms for controlling reinitiation events in the C period? RIDA and *datA* like control mechanisms as described for *E. coli* and other bacteria (Katayama *et al.*, 2010, Skarstad & Katayama, 2013) have not yet been described in mycobacteria. We propose that MtrA levels and phosphorylation activity are in part, responsible for controlling reinitiations in the C period. MtrB is the cognate sensor kinase that phosphorylates MtrA (Al Zayer et al., 2011, Plocinska et al., 2012). Thus, understanding the signals promoting MtrB activation, hence MtrA~P, during cell cycle will aid in unraveling the regulatory mechanisms impacting replication initiation. *PdnaA*, which contains MtrA- and DnaA- boxes, could exert another layer of control (Figs. S4 and 1 A), by acting as a sink to quench the active pools of DnaA remaining after initiation. Further studies are required to address these issues.

It is intriguing that *M. smegmatis oriC* is not a MtrA-target (Fig. 9). Also, the absence of F2-box did not affect *M. smegmatis oriC* plasmid transformation efficiency, growth and viability (see results). These data imply that either MtrA does not bind the lone F2 box of *M. smegmatis oriC* in vivo or the binding if any, has no biological consequences under the experimental conditions tested here. This begs two important but related questions: First, why is that the *M. tuberculosis oriC* evolved to be regulated by the MtrAB 2CRS? *M. tuberculosis* is a successful pathogen that can shift from an active multiplicative state to a chronic state in response to immune pressure. While the factors governing these processes are largely unknown, changes in the MtrA levels and its phosphorylation status are known to impact *M. tuberculosis* proliferation upon infection (Fol et al., 2006). Perhaps, regulation of the DnaA-mediated *ori*C replication along with other processes by the MtrA~P in response to immune/ environmental pressure is an adaptation strategy that *M. tuberculosis* uses for its optimal survival upon infection. Second, how is *M. smegmatis ori*C replication regulated? We suspect that either other yet to be identified proteins/factors and or MtrA interactions with DnaA and possibly other unidentified replisome components, contribute to the regulation of *M. smegmatis ori*C replication.

The MtrA-mediated regulation described here shares both similarities and differences with the known regulators in other organisms. For example, MtrA distinguishes itself from other regulators in that, unlike *E. coli* SeqA, the *ori*C sequestration process by MtrA is delayed until the D period (Skarstad & Katayama, 2013), and unlike Spo0A (Castilla-Llorente et al., 2006) and CtrA (Quon *et al.*, 1996, Quon et al., 1998) RRs, MtrA targets *dnaN* and *dnaA*, in addition to affecting the expression of other genes (Fig. 4). On the other hand, like the *B. subtilis* Soj, SirA, and YabA proteins (Murray & Errington, 2008, Noirot-Gros et al., 2006, Wagner et al., 2009), and HP1021 of *H. pylori* (Donczew et al., 2015) MtrA interacts with DnaA. The *dnaN* gene location, which is often adjacent to *oriC*, is well conserved in several bacteria (Gao *et al.*, 2013), and the *E. coli* and *C. cresentus* model organisms discussed here are exceptions. Also, the MtrAB 2CRS is conserved in high G+C rich actinobacteria such as *Corynebacterium glutamicum*, *C. diphtheria* and *Streptomyces sps* (Hoskisson & Hutchings, 2006). Thus, the MtrA-mediated regulation of *ori*C replication described here may extend to other eubacterial members having similar *ori*C organization and/or MtrA-like regulatory proteins.

Methods

Bacterial strains, culture conditions and molecular biology details

M. tuberculosis and *M. smegmatis* mc^{2}155 strains (Table S2) were propagated at 37°C in Middlebrook 7H9 broth supplemented with oleic acid-albumin-dextrose-catalase (OADC) or ADC, respectively as described (Plocinska et al., 2012). Actively growing *dna*Acos cultures were kept at 30°C for 30 h prior to shifting to 37°C for initiating synchronous replication as previously described (Nair et al., 2009). Where needed, *dna*Acos strains carrying plasmids expressing *mtr*A and its mutant derivatives were induced with 50 ng/mL *atc* added at the time of initiation of synchronous replication. Bacterial growth was assayed by measuring changes in absorbance at 600 nm, and viability by determining colony-forming units. The sequences of oligonucleotide primers used for cloning are given in Table S1. For some experiments, *M. smegmatis* transformed with *ori*C plasmids were plated for determining transformation efficiency as described (Qin et al., 1999, Qin et al., 1997).

MtrA-mCherry and MtrA$_{Y102C}$ proteins

Recombinant plasmid overexpressing his-*mtrA*--*mCherry* was created in three steps. First, *mCherry* coding region was amplified from pEB6 as *XbaI-SwaI* fragment using primers mCher_F_XbaI_lnkr and MR316_R_SwaI (Table S1). Second, *gfp* gene in the *mtrA-gfp* construct was replaced with *mCherry* (Table S2). Finally, the *mtrA-mCherry* coding region was amplified using primers MVM409F and mCher_R_XhoI (Table S1) and cloned into pET19b plasmid as *NdeI-XhoI* fragment for producing his-tagged protein. His-MtrA-mCherry was purified on Ni-NTA resin. Overproduction and purification of MtrA$_{Y102C}$-MBP was as described (Plocinska et al., 2012).

Chromatin immunoprecipitation (ChIP)-PCR

Formaldehyde cross-linked cultures of *M. tuberculosis* and *M. smegmatis* were used to perform ChIP-PCR using α-MtrA, α-DnaA or α-FtsZ antibodies, as described previously. The band intensities of each target were normalized to the non-target *Pfts*Z and genes with normalized values of 2 and above were considered as potential targets of MtrA or DnaA (Plocinska et al., 2012, Rajagopalan et al., 2010).

DNA synthesis and Western analysis

DNA synthesis was quantitated by measuring the incorporation of ^{3}H-uracil into alkali-stable DNA of uniformly labeled cells from samples collected in triplicate following initiation of synchronous replication as described (Nair et al., 2009). For Western analysis, cellular lysates of samples collected prior to and at various periods after the initiation of synchronous replication were prepared by bead beating and processed for immunoblotting with α-MtrA and α-SigA antibodies. Data were quantified using the volumetric analysis tool of the QuantityOne software and the MtrA/SigA ratios were determined as described (Fol et al., 2006, Plocinska et al., 2012).

Microscopy

*Mtb dna*Acos and *dna*Acos/MtrA$_{Y102C}$ at 0 and 48 h after the initiation of synchronous replication were fixed in 4% paraformaldehyde for 24 h, washed 3 times with PBS followed by incubation with propidium iodide stain (Molecular Probes) for 30 min at room temperature and visualized by brightfield and fluorescent imaging as described (Chauhan *et al.*, 2006).

Electrophoretic Mobility Shift Assay (EMSA)

A 526-bp fragment containing full-length *ori*C and 110-bp fragments bearing WT or mutant F2, F3, F4 and F5 MtrA-box motifs were amplified using 6-carboxyfluorescein (FITC)-labeled primers (Table S1) and WT (pMQ219) and mutant (pEBM12 and pEBM13) *oriC* plasmids (Table S2) as the templates. Mutant MtrA F2 box motif sequence TATATAC$_{CA}$TATATAT was as described (Rajagopalan et al., 2010). EMSA assays were performed with recombinant MtrA-mCherry (MtrA) and MtrA$_{Y102C}$-MBP preparations as described (Plocinska et al., 2012). Briefly, EnvZ was first autophosphorylated in a buffer containing 50 mM Tris-HCl, pH 7.5, 50 mM KCl, 20 mM $MgCl_2$, 1 mM DTT, 1 mM ATP at 37°C for 5 min prior to using in MtrA and MtrA$_{Y102C}$ transphosphorylation reactions. Next, FITC-labeled DNA (200 fmol) was incubated with increasing concentrations of phosphorylated or non-phosphorylated MtrA/MtrA$_{Y102C}$ along with poly(dI/dC) and sheared salmon sperm DNA for 15 min. The DNA-protein complexes were resolved in 5% polyacrylamide gels at 4°C, gels were scanned with a Molecular Imager (Fx) and data were analyzed using QuantityOne software (Plocinska et al., 2012, Rajagopalan et al., 2010). The percent *oriC* bound was calculated by quantifying free DNA in each well after appropriate background correction and subtraction from control (no MtrA) lanes (QuantityOne, BioRad). Apparent K_D and Hill-coefficient numbers were calculated using Prism 6 (Graphpad) software.

Solid phase *oriC* binding assays

Biotinylated *ori*C was PCR amplified using primers MVM257B/MVM1004 and template pMQ219 whereas biotinylated WT and mutant F2 MtrA-box sequences were amplified using primers MVM257B/MMtrF2R and templates pMQ219 and pMMR87, respectively (Rajagopalan et al., 2010). Approximately 10 μg biotinylated DNA and M270 Streptavidin magnetic beads were incubated with rocking for 3 h in buffer containing 5mM Tris-HCl, pH 7.5; 0.5 mM EDTA and 1M NaCl as per manufacturer's protocol (Invitrogen). Beads were magnetically separated from unbound DNA, washed and 2 μl beads were incubated with indicated concentrations of MtrA or MtrA$_{Y102C}$ in a 20 μl final volume at 37°C for 15 min. At the end of incubation, beads were collected, washed with 1× EMSA buffer, mixed with SDS-PAGE sample buffer and resolved by SDS-PAGE. Immunoblotting with α-MtrA was performed and the amount of bound MtrA was determined. As a control, *Pfts*Z was amplified using biotinylated oligo (ftsZP_F) and ftsZP_R and processed as described above. MtrA~P/MtrA ratios were calculated for 1.176 and 2.32 μM following densitometric analysis of data from two independent experiments.

RNA extraction and qRT-PCR

Extraction of total RNA from guanidine thiocyanate-fixed cells of *M. tuberculosis* followed by quantitative Real-Time PCR (qRT-PCR) for select genes were performed as described (Plocinska et al., 2012, Rajagopalan et al., 2010). QRT-PCR was performed in triplicate from three independent experiments in Bio-Rad iQ™5 iCycler Real-Time PCR detection system using FAM-labeled 2× iQ SYBR Supermix (Bio-rad, Cat# 1708880) as described. The primers used for qRT-PCR are listed in Table S1. The threshold cycle (*Ct*) value for each gene of interest was normalized to the *Ct* value of 16S rRNA, and the fold expression was calculated (fold change = $2^{-\Delta(\Delta Ct)}$) using the iQ™5 optical system software.

Protein-protein interaction assays: (i) Bacterial two hybrid (BACTH) assay

BACTH assays were performed using BATCH system kit (Euromedex) as described previously (Plocinski *et al.*, 2012). The MtrA and DnaA proteins were expressed as C-terminal fusions to *Bordetella pertussis* T18 or T25 adenylate cyclase fragments in the *E. coli* BTH101 strain (Tables S2). The co-transformants were spotted on minimal media agar supplemented with 0.004% X-gal, 100 μg/ml Amp and 50 μg/ml Km (Karimova *et al.*, 2005). The interaction strength was determined by measuring the extent of β-galactosidase activity in the broth-grown cultures (Plocinski et al., 2012). Beta-galactosidase activity of at least 5-fold or higher than that measured for *E. coli* BTH101 strain carrying single gene and empty vector was considered indicative of a positive interaction (Karimova et al., 2005). *E. coli* BTH101 transformants containing pKT25-GCN4 and pUT18C-GCN4 served as positive controls for complementation.

(2) Pull-down assays

Pull-down assays were performed to show interactions between DnaA and MtrA. Recombinant *M. smegmatis* bearing (pMMR41) or (pMG78) plasmids were induced with 0.2% acetamide for 6 hr to overproduce DnaA-His and MtrA respectively. The cell pellets were washed twice in 1× PBS, resuspended in lysis buffer containing 25 mM Tris-HCl pH 7.4, 150 mM NaCl, 1mM EDTA, 0.5% NP-40, 2.5% glycerol, 1mM PMSF and zirconia beads, beaten for 10× 30 sec and spun at 13, 200 rpm for 10 min to collect supernatant. Five hundred μL each of DnaA-His and MtrA lysates was mixed, pre-incubated at 4°C for 2 h followed by incubation with Ni-NTA resin for I h at 4°C. The Ni-NTA resin containing DnaA-His and MtrA was loaded onto spin column, washed 8× with 250 μL of lysis buffer, eluted with 50 μL buffer containing 300 mM imidazole and the collected fractions were analyzed by immunoblotting following SDS-PAGE.

Supplementary Material

Refer to Web version on PubMed Central for supplementary material.

Acknowledgements

We thank Drs. Dorota Stankowska for help with RvY102C and Naresh Arora with *M. smegmatis* ChIP experiments, Drs. Rao Lella and Susan Howard for helpful discussions, Dr. Sabine Ehrt for pTet plasmid system. This work was supported by NIH grants AI 084734 (MM) and AI 048417 (MR).

References

Al Zayer M, Stankowska D, Dziedzic R, Sarva K, Madiraju MV, Rajagopalan M. Mycobacterium tuberculosis mtrA merodiploid strains with point mutations in the signal-receiving domain of MtrA exhibit growth defects in nutrient broth. Plasmid. 2011; 65:210–218. [PubMed: 21295603]

Castilla-Llorente V, Munoz-Espin D, Villar L, Salas M, Meijer WJ. Spo0A, the key transcriptional regulator for entrance into sporulation, is an inhibitor of DNA replication. EMBO J. 2006; 25:3890–3899. [PubMed: 16888621]

Chauhan A, Lofton H, Maloney E, Moore J, Fol M, Madiraju MV, Rajagopalan M. Interference of Mycobacterium tuberculosis cell division by Rv2719c, a cell wall hydrolase. Mol Microbiol. 2006; 62:132–147. [PubMed: 16942606]

Cole ST, Brosch R, Parkhill J, Garnier T, Churcher C, Harris D, Gordon SV, Eiglmeier K, Gas S, Barry CE 3rd, Tekaia F, Badcock K, Basham D, Brown D, Chillingworth T, Connor R, Davies R, Devlin K, Feltwell T, Gentles S, Hamlin N, Holroyd S, Hornsby T, Jagels K, Krogh A, McLean J, Moule S, Murphy L, Oliver K, Osborne J, Quail MA, Rajandream MA, Rogers J, Rutter S, Seeger K, Skelton J, Squares R, Squares S, Sulston JE, Taylor K, Whitehead S, Barrell BG. Deciphering the biology of Mycobacterium tuberculosis from the complete genome sequence. Nature. 1998; 393:537–544. [PubMed: 9634230]

Cooper S, Helmstetter CE. Chromosome replication and the division cycle of Escherichia coli B/r. J Mol Biol. 1968; 31:519–540. [PubMed: 4866337]

Dick T, Lee BH, Murugasu-Oei B. Oxygen depletion induced dormancy in Mycobacterium smegmatis. FEMS Microbiol Lett. 1998; 163:159–164. [PubMed: 9673018]

Domian IJ, Quon KC, Shapiro L. Cell type-specific phosphorylation and proteolysis of a transcriptional regulator controls the G1-to-S transition in a bacterial cell cycle. Cell. 1997; 90:415–424. [PubMed: 9267022]

Donczew R, Makowski L, Jaworski P, Bezulska M, Nowaczyk M, Zakrzewska-Czerwinska J, Zawilak-Pawlik A. The atypical response regulator HP1021 controls formation of the Helicobacter pylori replication initiation complex. Mol Microbiol. 2015; 95:297–312. [PubMed: 25402746]

Ehrt S, Guo XV, Hickey CM, Ryou M, Monteleone M, Riley LW, Schnappinger D. Controlling gene expression in mycobacteria with anhydrotetracycline and Tet repressor. Nucleic Acids Res. 2005; 33:e21. [PubMed: 15687379]

Fol M, Chauhan A, Nair NK, Maloney E, Moomey M, Jagannath C, Madiraju MV, Rajagopalan M. Modulation of Mycobacterium tuberculosis proliferation by MtrA, an essential two-component response regulator. Mol Microbiol. 2006; 60:643–657. [PubMed: 16629667]

Friedland N, Mack TR, Yu M, Hung LW, Terwilliger TC, Waldo GS, Stock AM. Domain orientation in the inactive response regulator Mycobacterium tuberculosis MtrA provides a barrier to activation. Biochemistry. 2007; 46:6733–6743. [PubMed: 17511470]

Galagan JE, Minch K, Peterson M, Lyubetskaya A, Azizi E, Sweet L, Gomes A, Rustad T, Dolganov G, Glotova I, Abeel T, Mahwinney C, Kennedy AD, Allard R, Brabant W, Krueger A, Jaini S, Honda B, Yu WH, Hickey MJ, Zucker J, Garay C, Weiner B, Sisk P, Stolte C, Winkler JK, Van de Peer Y, Iazzetti P, Camacho D, Dreyfuss J, Liu Y, Dorhoi A, Mollenkopf HJ, Drogaris P, Lamontagne J, Zhou Y, Piquenot J, Park ST, Raman S, Kaufmann SH, Mohney RP, Chelsky D, Moody DB, Sherman DR, Schoolnik GK. The Mycobacterium tuberculosis regulatory network and hypoxia. Nature. 2013; 499:178–183. [PubMed: 23823726]

Gao F, Luo H, Zhang CT. DoriC 5.0: an updated database of oriC regions in both bacterial and archaeal genomes. Nucleic Acids Res. 2013; 41:D90–D93. [PubMed: 23093601]

Gill WP, Harik NS, Whiddon MR, Liao RP, Mittler JE, Sherman DR. A replication clock for Mycobacterium tuberculosis. Nat Med. 2009; 15:211–214. [PubMed: 19182798]

Gorbatyuk B, Marczynski GT. Regulated degradation of chromosome replication proteins DnaA and CtrA in Caulobacter crescentus. Mol Microbiol. 2005; 55:1233–1245. [PubMed: 15686567]

Hoskisson PA, Hutchings MI. MtrAB-LpqB: a conserved three-component system in actinobacteria? Trends Microbiol. 2006; 14:444–449. [PubMed: 16934981]

Karimova G, Dautin N, Ladant D. Interaction network among Escherichia coli membrane proteins involved in cell division as revealed by bacterial two-hybrid analysis. J Bacteriol. 2005; 187:2233–2243. [PubMed: 15774864]

Katayama T, Ozaki S, Keyamura K, Fujimitsu K. Regulation of the replication cycle: conserved and diverse regulatory systems for DnaA and oriC. Nat Rev Microbiol. 2010; 8:163–170. [PubMed: 20157337]

Keyamura K, Fujikawa N, Ishida T, Ozaki S, Su'etsugu M, Fujimitsu K, Kagawa W, Yokoyama S, Kurumizaka H, Katayama T. The interaction of DiaA and DnaA regulates the replication cycle in E. coli by directly promoting ATP DnaA-specific initiation complexes. Genes Dev. 2007; 21:2083–2099. [PubMed: 17699754]

Kumar S, Farhana A, Hasnain SE. In-vitro helix opening of M. tuberculosis oriC by DnaA occurs at precise location and is inhibited by IciA like protein. PLoS One. 2009; 4:e4139. [PubMed: 19127296]

Lee YS, Han JS, Jeon Y, Hwang DS. The arc two-component signal transduction system inhibits in vitro Escherichia coli chromosomal initiation. J Biol Chem. 2001; 276:9917–9923. [PubMed: 11133990]

Li Y, Zeng J, Zhang H, He ZG. The characterization of conserved binding motifs and potential target genes for M. tuberculosis MtrAB reveals a link between the two-component system and the drug resistance of M. smegmatis. BMC Microbiol. 2010; 10:242. [PubMed: 20843371]

Lim A, Eleuterio M, Hutter B, Murugasu-Oei B, Dick T. Oxygen depletion-induced dormancy in Mycobacterium bovis BCG. J Bacteriol. 1999; 181:2252–2256. [PubMed: 10094705]

Madiraju MV, Moomey M, Neuenschwander PF, Muniruzzaman S, Yamamoto K, Grimwade JE, Rajagopalan M. The intrinsic ATPase activity of Mycobacterium tuberculosis DnaA promotes rapid oligomerization of DnaA on oriC. Mol Microbiol. 2006; 59:1876–1890. [PubMed: 16553890]

Murray H, Errington J. Dynamic control of the DNA replication initiation protein DnaA by Soj/ParA. Cell. 2008; 135:74–84. [PubMed: 18854156]

Nair N, Dziedzic R, Greendyke R, Muniruzzaman S, Rajagopalan M, Madiraju MV. Synchronous replication initiation in novel Mycobacterium tuberculosis dnaA cold-sensitive mutants. Mol Microbiol. 2009; 71:291–304. [PubMed: 19019143]

Nguyen HT, Wolff KA, Cartabuke RH, Ogwang S, Nguyen L. A lipoprotein modulates activity of the MtrAB two-component system to provide intrinsic multidrug resistance, cytokinetic control and cell wall homeostasis in Mycobacterium. Mol Microbiol. 2010; 76:348–364. [PubMed: 20233304]

Noirot-Gros MF, Velten M, Yoshimura M, McGovern S, Morimoto T, Ehrlich SD, Ogasawara N, Polard P, Noirot P. Functional dissection of YabA, a negative regulator of DNA replication initiation in Bacillus subtilis. Proc Natl Acad Sci U S A. 2006; 103:2368–2373. [PubMed: 16461910]

Plocinska R, Purushotham G, Sarva K, Vadrevu IS, Pandeeti EV, Arora N, Plocinski P, Madiraju MV, Rajagopalan M. Septal Localization of the Mycobacterium tuberculosis MtrB Sensor Kinase Promotes MtrA Regulon Expression. J Biol Chem. 2012; 287:23887–23899. [PubMed: 22610443]

Plocinski P, Arora N, Sarva K, Blaszczyk E, Qin H, Das N, Plocinska R, Ziolkiewicz M, Dziadek J, Kiran M, Gorla P, Cross TA, Madiraju M, Rajagopalan M. Mycobacterium tuberculosis CwsA interacts with CrgA and Wag31 and the CrgA-CwsA complex is involved in peptidoglycan synthesis and cell shape determination. J Bacteriol. 2012

Qin MH, Madiraju MV, Rajagopalan M. Characterization of the functional replication origin of Mycobacterium tuberculosis. Gene. 1999; 233:121–130. [PubMed: 10375628]

Qin MH, Madiraju MV, Zachariah S, Rajagopalan M. Characterization of the oriC region of Mycobacterium smegmatis. J Bacteriol. 1997; 179:6311–6317. [PubMed: 9335277]

Quon KC, Marczynski GT, Shapiro L. Cell cycle control by an essential bacterial two-component signal transduction protein. Cell. 1996; 84:83–93. [PubMed: 8548829]

Quon KC, Yang B, Domian IJ, Shapiro L, Marczynski GT. Negative control of bacterial DNA replication by a cell cycle regulatory protein that binds at the chromosome origin. Proc Natl Acad Sci U S A. 1998; 95:120–125. [PubMed: 9419339]

Rajagopalan M, Dziedzic R, Al Zayer M, Stankowska D, Ouimet MC, Bastedo DP, Marczynski GT, Madiraju MV. Mycobacterium tuberculosis origin of replication and the promoter for immunodominant secreted antigen 85B are the targets of MtrA, the essential response regulator. J Biol Chem. 2010; 285:15816–15827. [PubMed: 20223818]

Rand L, Hinds J, Springer B, Sander P, Buxton RS, Davis EO. The majority of inducible DNA repair genes in Mycobacterium tuberculosis are induced independently of RecA. Mol Microbiol. 2003; 50:1031–1042. [PubMed: 14617159]

Salazar L, Fsihi H, de Rossi E, Riccardi G, Rios C, Cole ST, Takiff HE. Organization of the origins of replication of the chromosomes of Mycobacterium smegmatis, Mycobacterium leprae and Mycobacterium tuberculosis and isolation of a functional origin from M. smegmatis. Mol Microbiol. 1996; 20:283–293. [PubMed: 8733228]

Salazar L, Guerrero E, Casart Y, Turcios L, Bartoli F. Transcription analysis of the dnaA gene and oriC region of the chromosome of Mycobacterium smegmatis and Mycobacterium bovis BCG, and its regulation by the DnaA protein. Microbiology. 2003; 149:773–784. [PubMed: 12634345]

Santi I, Dhar N, Bousbaine D, Wakamoto Y, McKinney JD. Single-cell dynamics of the chromosome replication and cell division cycles in mycobacteria. Nature communications. 2013; 4:2470.

Skarstad K, Katayama T. Regulating DNA replication in bacteria. Cold Spring Harbor perspectives in biology. 2013; 5:a012922. [PubMed: 23471435]

Smith I. Mycobacterium tuberculosis pathogenesis and molecular determinants of virulence. Clin Microbiol Rev. 2003; 16:463–496. [PubMed: 12857778]

Smollett KL, Smith KM, Kahramanoglou C, Arnvig KB, Buxton RS, Davis EO. Global analysis of the regulon of the transcriptional repressor LexA, a key component of SOS response in Mycobacterium tuberculosis. J Biol Chem. 2012; 287:22004–22014. [PubMed: 22528497]

Trojanowski D, Ginda K, Pioro M, Holowka J, Skut P, Jakimowicz D, Zakrzewska-Czerwinska J. Choreography of the Mycobacterium replication machinery during the cell cycle. mBio. 2015; 6:e02125–e02114. [PubMed: 25691599]

van Kessel JC, Hatfull GF. Efficient point mutagenesis in mycobacteria using single-stranded DNA recombineering: characterization of antimycobacterial drug targets. Mol Microbiol. 2008; 67:1094–1107. [PubMed: 18221264]

Wagner JK, Marquis KA, Rudner DZ. SirA enforces diploidy by inhibiting the replication initiator DnaA during spore formation in Bacillus subtilis. Mol Microbiol. 2009; 73:963–974. [PubMed: 19682252]

Wayne LG. Synchronized replication of Mycobacterium tuberculosis. Infect Immun. 1977; 17:528–530. [PubMed: 409675]

Yamamoto K, Muniruzzaman S, Rajagopalan M, Madiraju MV. Modulation of Mycobacterium tuberculosis DnaA protein-adenine-nucleotide interactions by acidic phospholipids. Biochem J. 2002; 363:305–311. [PubMed: 11931658]

Zahrt TC, Deretic V. An essential two-component signal transduction system in Mycobacterium tuberculosis. J Bacteriol. 2000; 182:3832–3838. [PubMed: 10851001]

Zawilak A, Kois A, Konopa G, Smulczyk-Krawczyszyn A, Zakrzewska-Czerwinska J. Mycobacterium tuberculosis DnaA initiator protein: purification and DNA-binding requirements. Biochem J. 2004; 382:247–252. [PubMed: 15137907]

Zawilak-Pawlik A, Kois A, Stingl K, Boneca IG, Skrobuk P, Piotr J, Lurz R, Zakrzewska-Czerwinska J, Labigne A. HobA--a novel protein involved in initiation of chromosomal replication in Helicobacter pylori. Mol Microbiol. 2007; 65:979–994. [PubMed: 17645450]

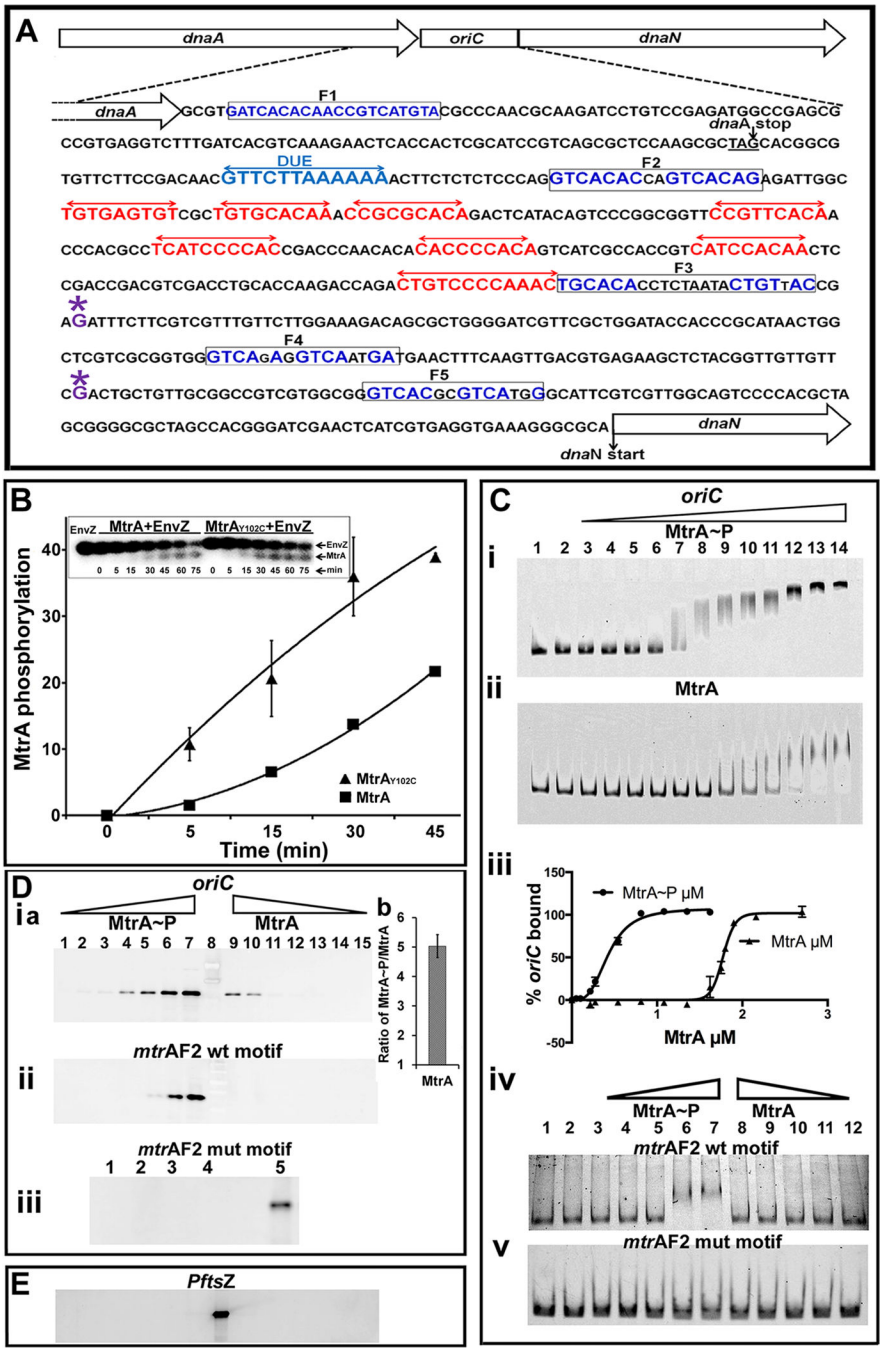

Fig. 1.

(A) *M. tuberculosis oriC* region and *oriC* sequence with DnaA- and MtrA- boxes. The *dna*A-*dna*N intergenic region of *M. tuberculosis* containing DnaA-boxes (red double arrows), MtrA-motifs (boxed) and DUE sequence (blue double arrows) is shown. For clarity, only the DnaA-boxes defined based on our earlier DMS footprinting data are shown (Madiraju et al., 2006). Although not shown, DNaseI footprinting data located two additional boxes in the 3' end of *oriC*, presumably these are low-affinity DnaA- boxes (Zawilak *et al.*, 2004). Presumptive transcription start sites at −110 (downstream of F4 box)

and −258 (downstream of F3 box) relative to *dnaN* start codon based on *M. bovis* BCG sequence are marked with '*' above the 'G' residue (Salazar et al., 2003). **(B)** Kinetics of MtrA phosphorylation. Autophosphorylated EnvZ was incubated with MtrA or $MtrA_{Y102C}$, samples at indicated time periods were removed, resolved by SDS-PAGE, autoradiography was performed, signals were quantitated by densitometry on a Bio-Rad Molecular imager and data plotted. Inset shows a representative SDS-PA gel autoradiograph image of radiolabeled MtrA and EnvZ proteins. **(C)** EMSA showing MtrA binding to *oriC* (panels i, ii) and DNA fragments containing MtrA F2 WT and mutant sequences (panels iv, v). Lanes 1 and 2 (panels i– v) are controls wherein DNA alone (lane 1) or that incubated with EnvZ in the absence of MtrA (lane 2) were resolved. MtrA-mCherry~P was used at 0.054, 0.108, 0.216, 0.27, 0.54, 0.81, 1.35, 1.62, 1.89, 2.16 and 2.7 μM (panels C-i) and MtrA-mCherry at 0.216, 0.27, 0.54, 0.81, 1.08, 1.35, 1.62, 1.75, 1.8, 1.9, 2.16 and 2.7 μM (panels C-ii). Binding data were quantified and the percent *oriC* bound was calculated (panel iii). MtrA-binding to F2 WT (panel iv) and mutant sequence (panel v) were performed at 0.27, 0.54, 1.08, 2.16 and 2.7 μM protein concentration. **(D)** Solid phase DNA-binding assays. Streptavidin magnetic beads conjugated with biotinylated *oriC* (panel i) or MtrA F2 box sequences (panels ii, iii) were incubated with MtrA and processed as described in methods section. MtrA proteins were used at 0.0365, 0.0735, 0.147, 0.294, 0.588, 1.176, 2.32 μM. MtrA~P or MtrA bound to *oriC* was determined by densitometry and MtrA~P/MtrA calculated for 1.176, 2.32 μM (Panel D-i b). Binding experiments with MtrA-F2 mutant box sequence were performed in duplicate at 1.176 μM (panel D-iii, lanes 1 and 2) and 2.32 μM MtrA (panel D-iii, lanes 3 and 4) respectively, as other concentrations did not show any binding. **(E)** Binding assays were performed with *PftsZ* and immunoblotted with α-MtrA as described above. All binding conditions were similar to *oriC* (D-i). *Note:* Lanes '8' in D-i a and E and '5' in D-iii are positive controls wherein streptavidin beads conjugated to *oriC* or MtrA F2 box, respectively, were incubated with 1. 176 μM MtrA~P.

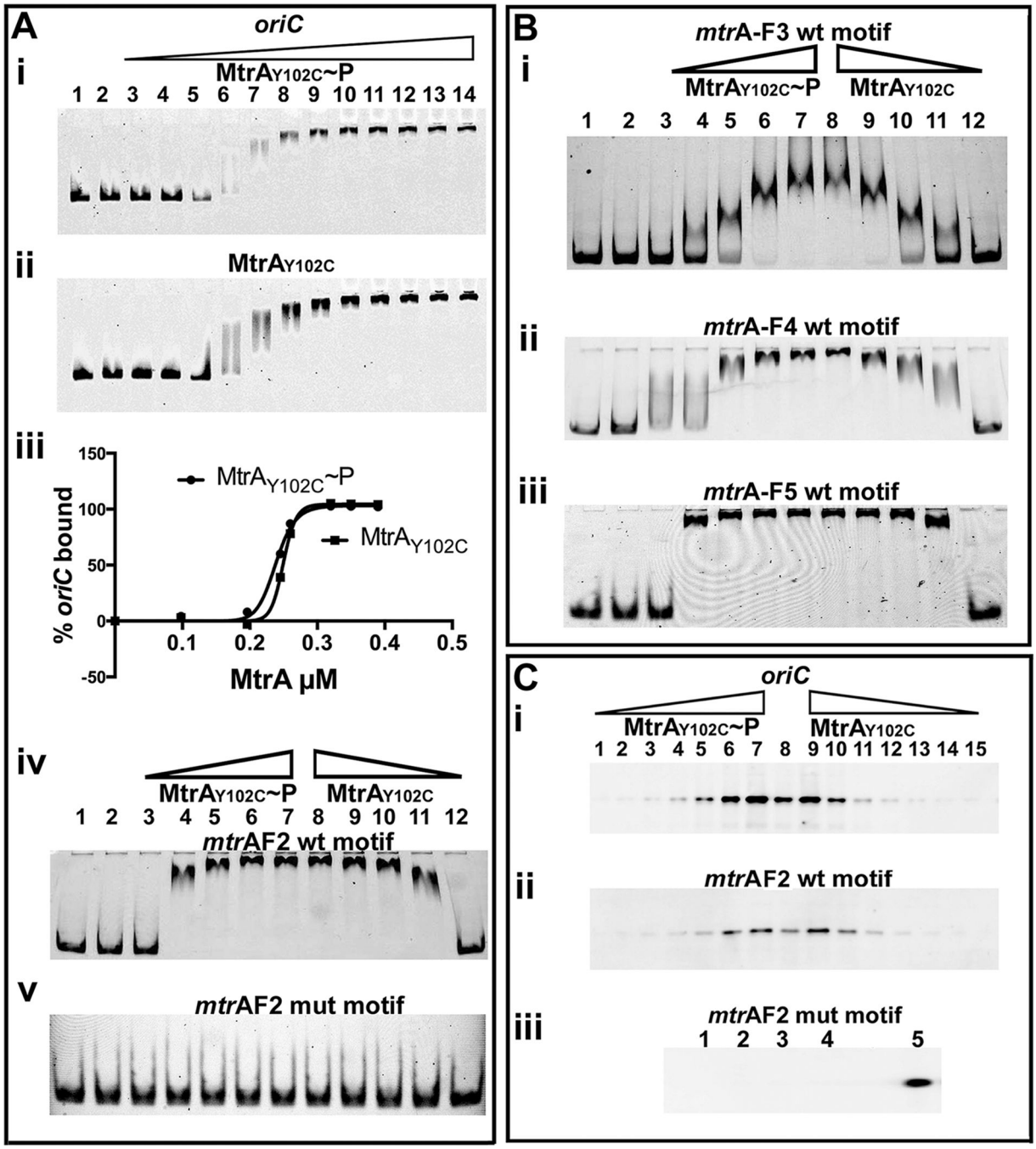

Fig. 2.

(A) EMSA showing $MtrA_{Y102C}$ binding to *oriC* and F2 box sequences. Lanes 1 and 2 (panels i, ii, iv and v) are MtrA controls wherein DNA was incubated with (lane 1) or without (lane 2) EnvZ and electrophoresed. $MtrA_{Y102C}$~P (panel A-i) or $MtrA_{Y102C}$ (panel A-ii) was used at 0.098, 0.196, 0.245, 0.294, 0.343, 0.392, 0.784, 1.76, 1.96, 2.45, 2.94 and 3.43 µM. Binding data were quantified and plotted (panel- iii). $MtrA_{Y102C}$ binding to MtrA F2 WT (panel iv) and mutant box (panel v) fragments were assayed at 0.196, 0.392, 0.784, 1.176 and 1.96 µM in ascending (lanes 3 to 7) and descending (8 to 12) order of protein

concentration, respectively. **(B)** $MtrA_{Y102C}$ binding to MtrA-boxes F3, F4 and F5. All experimental conditions including the controls are as described in 'A'. **(C)** Solid-phase DNA binding assay: $MtrA_{Y102C}$~P or $MtrA_{Y102C}$ binding to biotinylated *oriC* (panels i) or MtrA F2 fragments (panels ii,iii) was determined as described under Fig. 1 D at 0.049, 0.098, 0.196, 0.392, 0.784, 1.568, 3.136 μM concentrations. Data shown are in increasing order of protein concentration for $MtrA_{Y102C}$~P and decreasing order for $MtrA_{Y102C}$. $MtrA_{Y102C}$~P binding to F2 mutant MtrA-box was assayed at 1.568 (lanes 1 and 2) and 3.136 μM (lanes 3 and 4), respectively. *Note:* Lanes '8' in C-i/ii and '5' in C-iii are positive controls wherein streptavidin beads conjugated to *oriC* or MtrA F2 box, respectively, were incubated with 1. 568 μM MtrA~P.

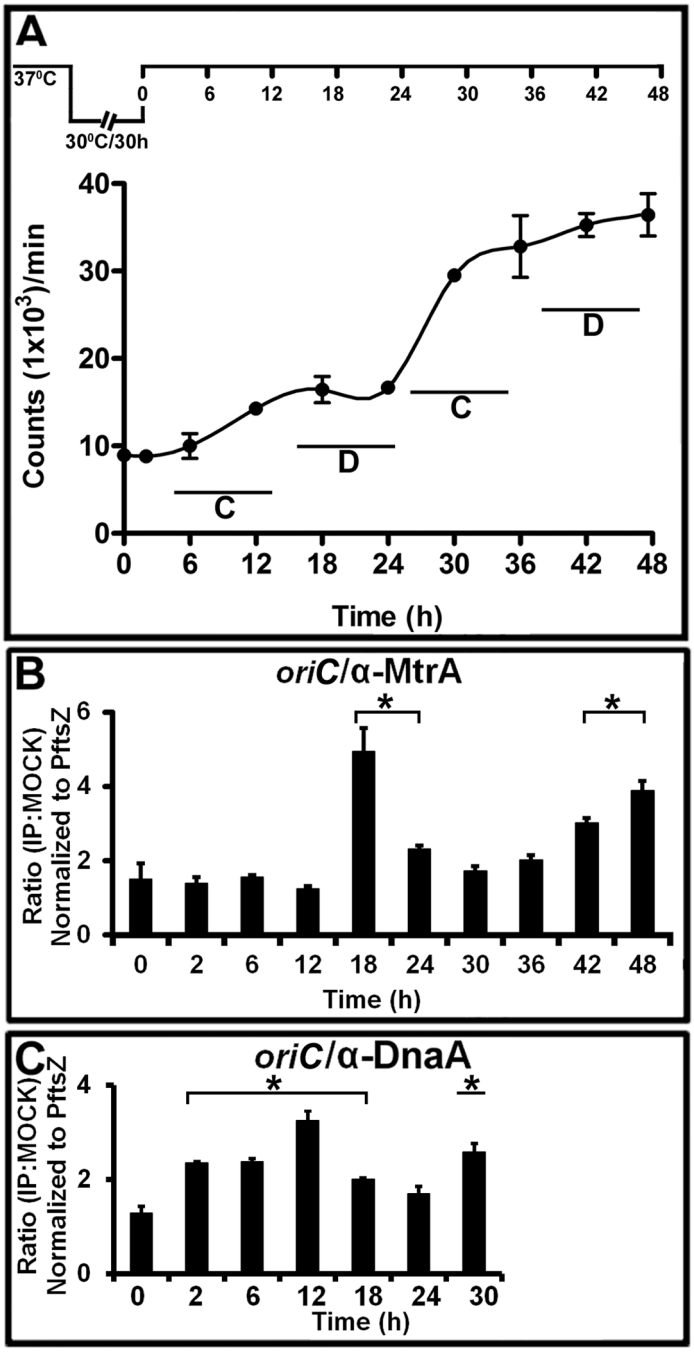

Fig. 3.

The MtrA and DnaA occupancy of *ori*C in synchronously replicating cultures. (A) DNA synthesis was measured as ^{3}H-uracil incorporation, normalized to OD_{600}=1 and presented as counts per minute (CPM) on the Y-axis. The X-axis shows the time periods when samples were processed. The C and D periods are marked for clarity. A typical *dna*Acos synchronization plan is also shown at the top of this panel. (B) ChIP-PCR assay showing the MtrA occupancy of *ori*C during the cell cycle. The ChIP assay was performed at the indicated time points with α-MtrA followed by PCR of *ori*C (MtrA target) and *Pfts*Z (non-

target). The ratio of IP to the mock signal was determined for each time point, normalized against the *Pfts*Z promoter value and shown on the Y-axis. The p-values were calculated by Student's unpaired t-test and * denotes a p-value ≤0.05 for samples showing significant enrichment of 2 and above. (C) ChIP-PCR assay showing the DnaA occupancy of *ori*C during the cell cycle. All experimental conditions and details as described in 'B' except that DnaA antibodies were used to process samples.

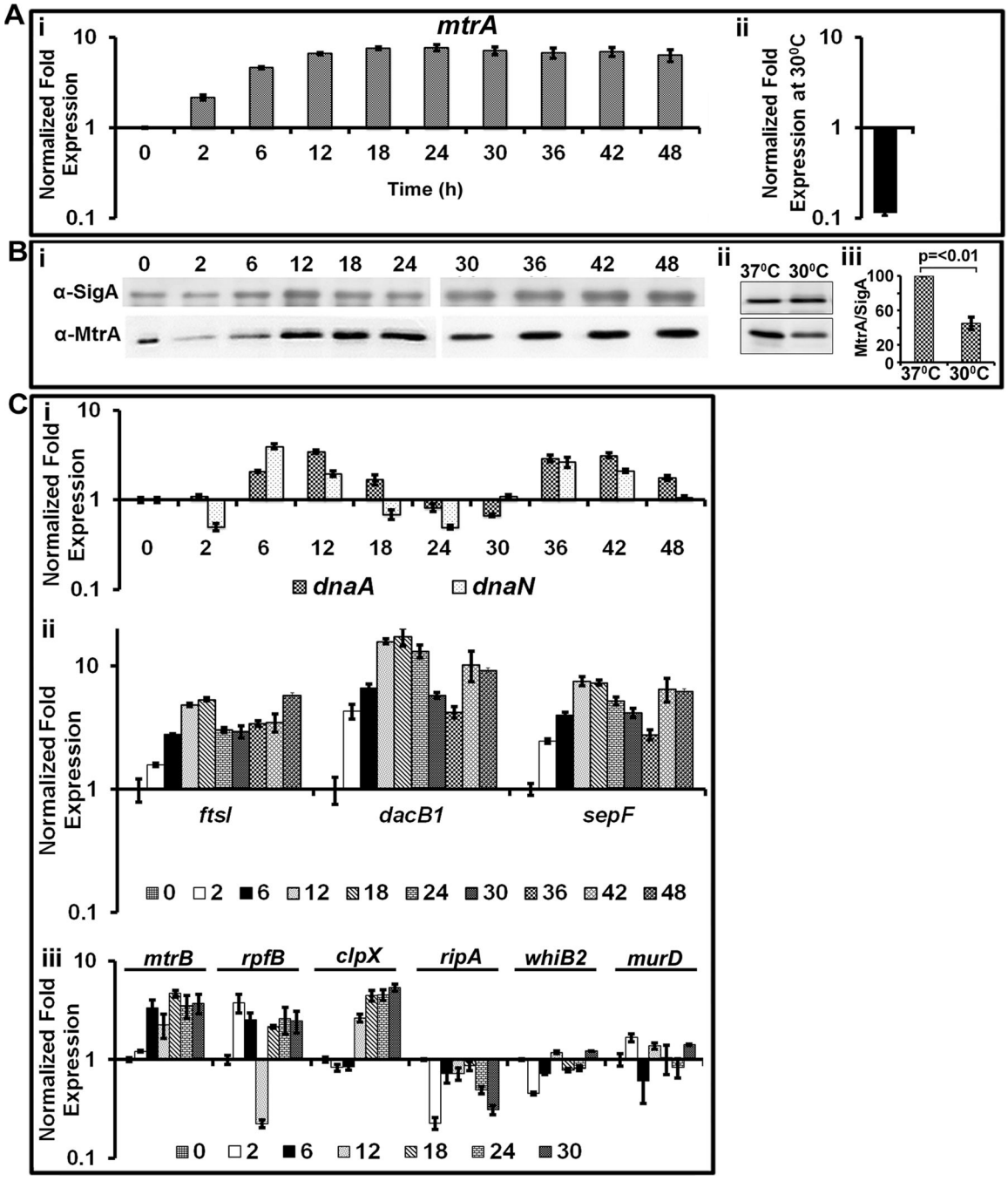

Fig. 4.

Evaluation of the *mtr*A transcript, protein and select target expression as a function of cell cycle. (A) qRT-PCR analysis of *mtr*A transcript levels: Panel i: Total RNA from synchronously replicating cultures of *M. tuberculosis dna*Acos at the indicated time points were extracted and the expression levels of 16S rRNA and *mtr*A were determined. Data shown are normalized to 16SrRNA and fold expression relative to 30°C is shown. Panel **ii** shows *mtr*A expression levels in *dna*Acos grown at 30°C for 30 h and normalized against that actively growing at 37°C. (B) Immunoblots showing MtrA and SigA: Total proteins

were extracted from synchronously replicating *dna*Acos samples at indicated time periods, probed with α-MtrA and α-SigA to determine expression levels of MtrA during cell cycle. Note: Two micrograms of lysates were loaded for each time point except for 0 h sample, for which 5 μg of lysate was loaded to detect MtrA as its concentration was reduced under non-growing conditions. Panel **ii**- immunoblots showing MtrA and SigA in *Mtb dna*Acos grown at 30°C for 30 h and actively growing cultures at 37°C. Panel iii: MtrA and SigA band intensities of panel ii were determined, the MtrA/SigA ratio and the p-value were determined from three independent experiments. (C) qRT-pCR analysis of select MtrA-targets normalized to that of 16S rRNA. Panel i: expression profiles of *dnaN* and *dnaA*; Panel ii: expression profiles of *ftsI, dacB1* and *sep*F; Panel iii; expression profiles of targets *rpfB, ripA, whiB2, clpX* and non-targets *murD* and *mtrB*.

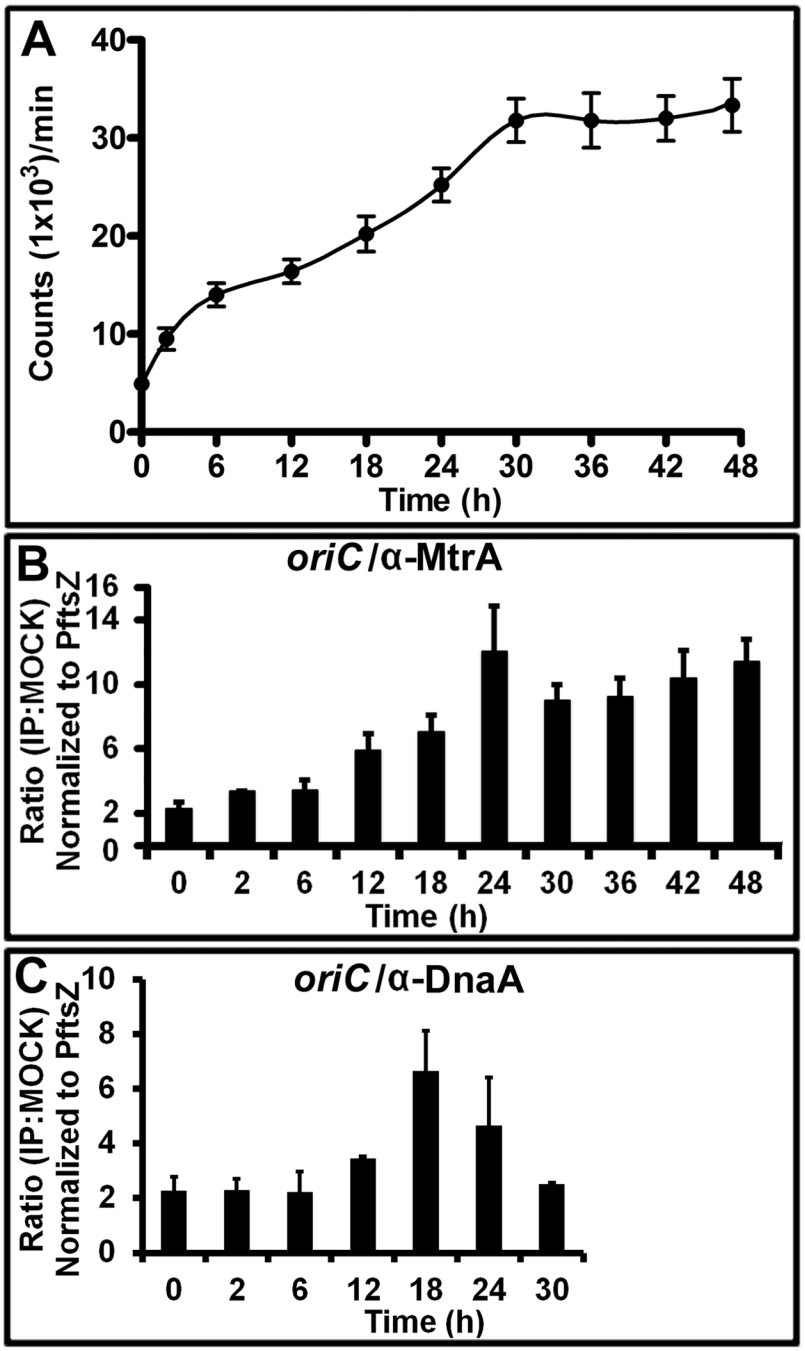

Fig. 5.

DNA synthesis and *oriC* occupancy of MtrA and DnaA in *dna*Acos/MtrA$_{Y102C}$. The inducer '*atc*' was added at the time of initiation of synchronous replication (0 h) to overproduce MtrA$_{Y102C}$. (A). DNA synthesis determined as described under Fig. 3A. (B). ChIP-PCR showing the MtrA occupancy of *oriC* performed as described for Fig. 3B. (C) ChIP-PCR showing the DnaA occupancy of *oriC* as described for Fig. 3C.

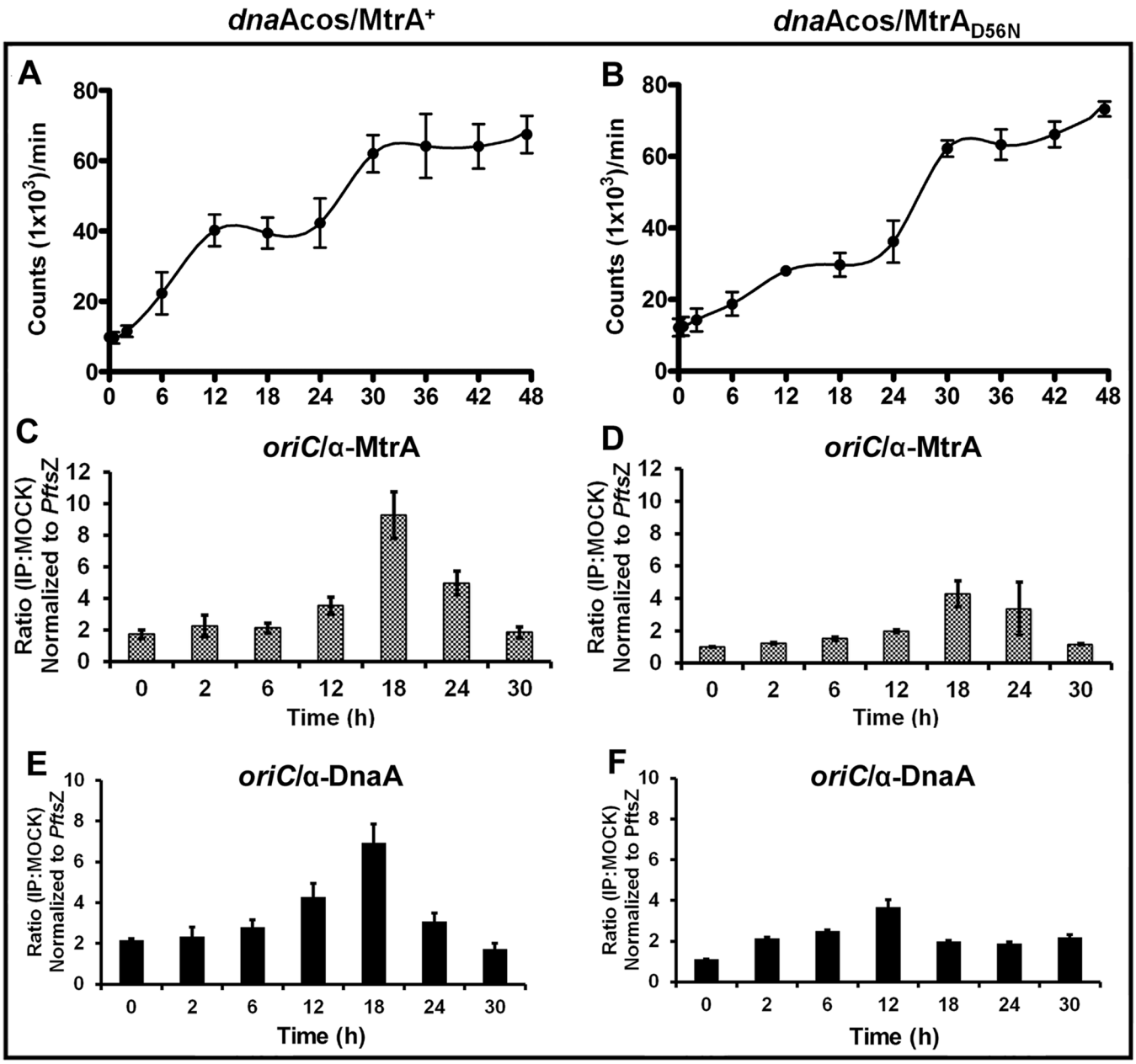

Fig. 6.

Characterization of *dna*Acos/MtrA+ and *dna*Acos/MtrA$_{D56N}$. DNA synthesis in *dna*Acos/MtrA+ (A) and *dna*Acos/MtrA$_{D56N}$ (B). All experimental details are as described under Fig. 3A. MtrA occupancy of *oriC* in *dna*Acos/MtrA+ (C) and *dna*Acos/MtrA$_{D56N}$ (D). ChIP-PCR was performed following IP with MtrA antibodies as described under Fig. 3B. DnaA occupancy of *oriC* in *dna*Acos/MtrA+ (E) and *dna*Acos/MtrA$_{D56N}$ (F). ChIP-PCR was performed following IP with DnaA antibodies as described under Fig. 3C.

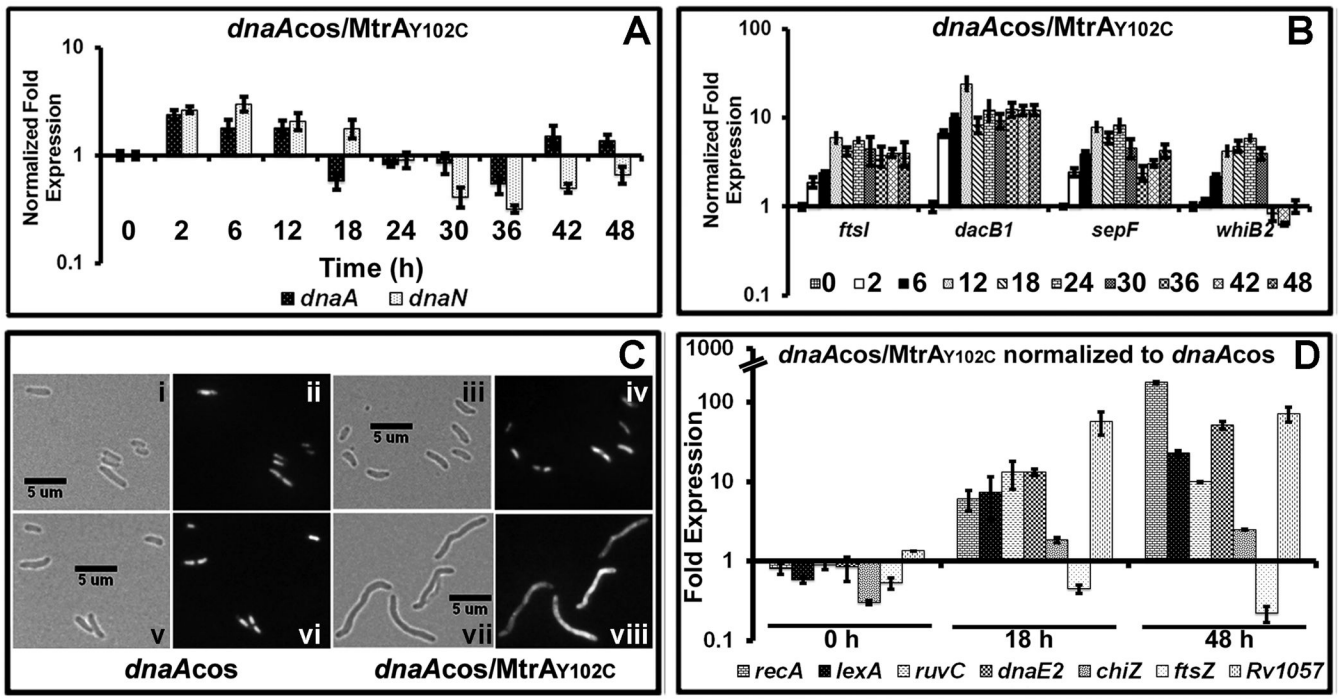

Fig. 7.

Characterization of *dna*Acos/MtrA$_{Y102C}$: (A) qRT-PCR analysis of select MtrA targets. Total RNA was extracted from *dna*Acos/*mtr*A$_{Y102C}$ at indicated time points and fold expression relative to 16S rRNA was calculated as described in Fig. 4A. (B) qRT-PCR analysis of select cell-division targets *fts*I, *dac*B1, *sep*F and *whi*B2 relative to 16S rRNA. (C) Cell morphology of *dna*Acos and *dna*Acos/MtrA$_{Y102C}$: The *dna*Acos (panels i, ii, v, vi) and *dna*Acos/MtrA$_{Y102C}$ (panels iii, iv, vii, viii) cultures were visualized by microscopy at 0 h (i– iv) and 48 (v– viii) h after initiation of synchronous replication. Brightfield (i, iii, v, vii) and respective fluorescence images obtained following propidium iodide staining (ii, iv, vi, viii) are shown. **(D)** qRT-PCR analysis of SOS target gene expression. Total RNA from synchronously replicating cultures of *M. tuberculosis dna*Acos and *dna*Acos/MtrA$_{Y102C}$ at indicated time points was extracted and the expression levels of *rec*A, *lex*A, *ruv*C, *dna*E2, *chi*Z *fts*Z and Rv1057 were determined. Data were normalized to 16SrRNA and fold expression relative to 30°C was determined. Final fold expression was calculated by normalizing *dna*Acos/MtrA$_{Y102C}$ expression at 0, 18 and 48 h to the respective time points of *dna*Acos.

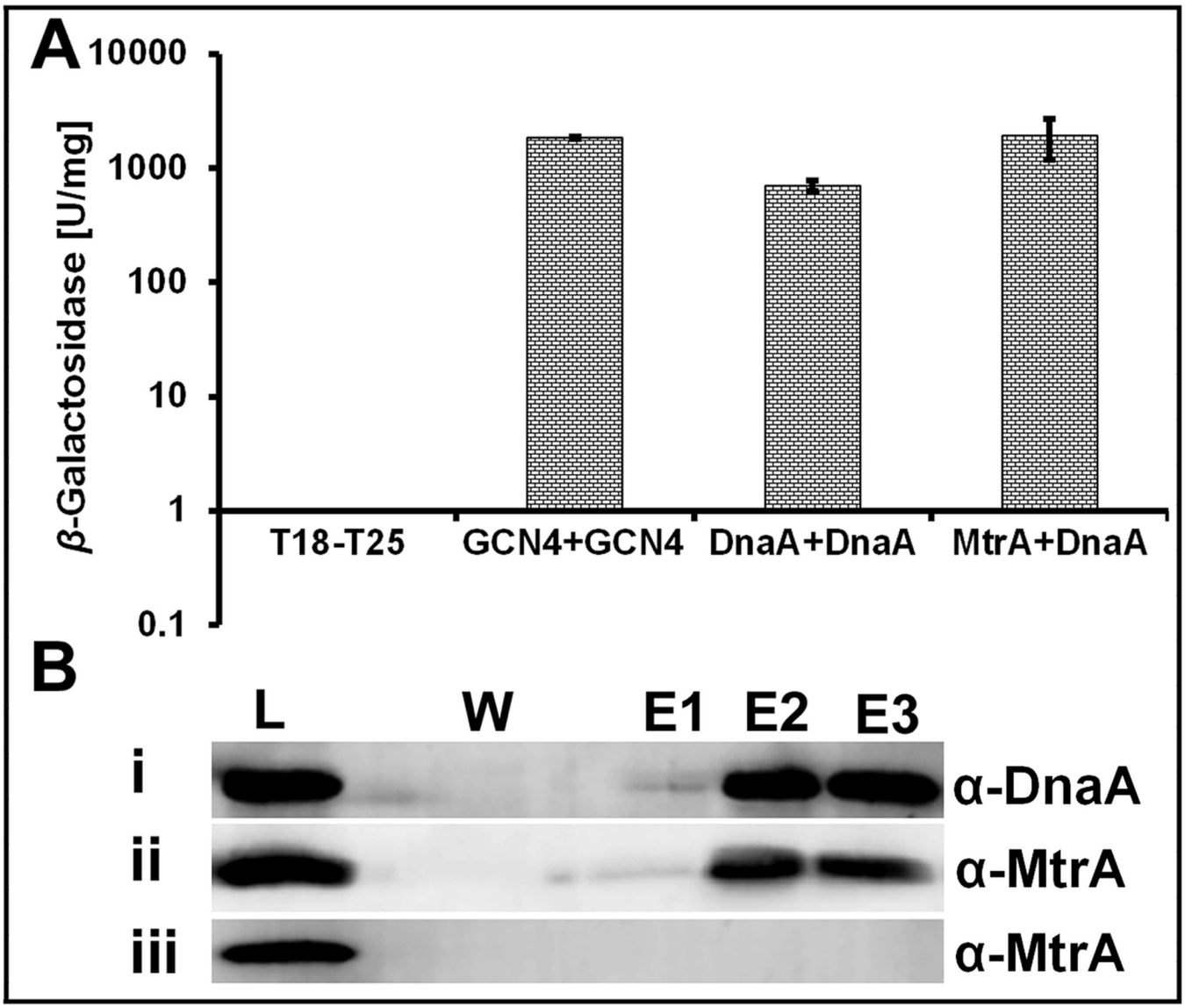

Fig. 8. BACTH and Pull-down assays

(A) BACTH analysis showing the interaction between MtrA and DnaA in *E. coli*. Strength of interactions is presented as β-galactosidase units per milligram protein as described under methods. GCN4-GCN4 is positive control. Mean ± SD values from three independent experiments are shown. (B) Immunoblots showing pull-down of DnaA and MtrA proteins. *M. smegmatis* lysates containing DnaA-His and MtrA were mixed and processed for pull-down reaction on Ni-NTA resin as described in text. Eluted proteins were examined following immunoblotting with DnaA (panel i) and MtrA (panel ii) antibodies. Pull-down reaction with *M. smegmatis* MtrA lysate was performed and eluted samples were probed with MtrA antibodies (panel iii). W refers to the sample collected after washing the resin 8× with buffer containing 20 mM imidazole whereas E1, E2 and E3 are elutions with 300 mM imidazole. L= load. Note - panel iii lane corresponding to W does not contain MtrA although wash sample 1 contained MtrA (data not shown).

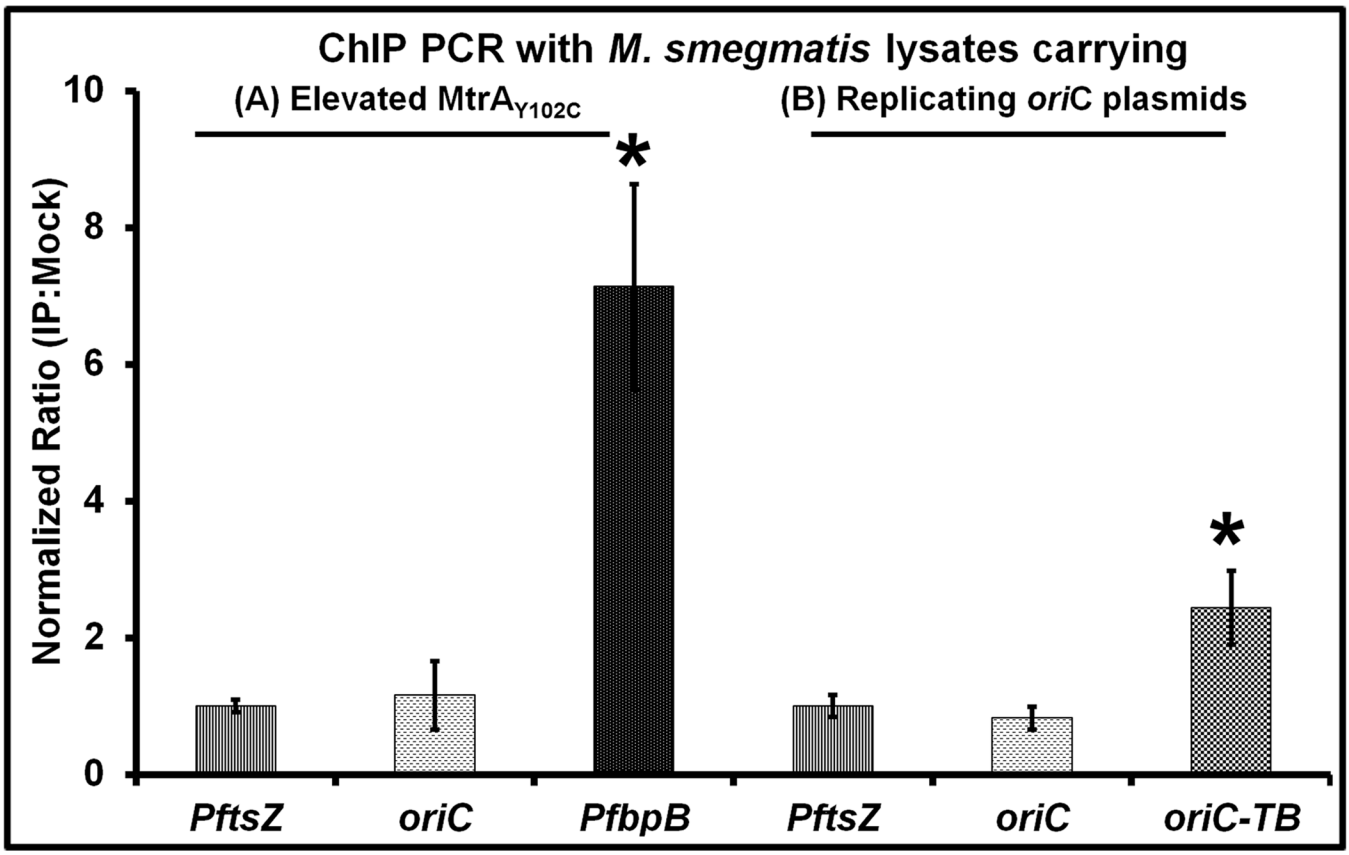

Fig. 9.

ChIP-PCR studies with *M. smegmatis* lysates. (A) *M. smegmatis* producing MtrA$_{Y102C}$ were processed for ChIP studies with MtrA antibodies essentially as described for Fig. 3C. Following the reversal of cross-links, PCR was performed for MtrA-targets *oriC* and *PfbpB* and the non-target *Pfts*Z. (B) ChIP-PCR with *M. smegmatis* lysates carrying the *M. smegmatis oriC* (pMQ131) (Qin et al., 1997) and *M. tuberculosis oriC* (pMQ219) (Qin et al., 1999) in replicating plasmids.

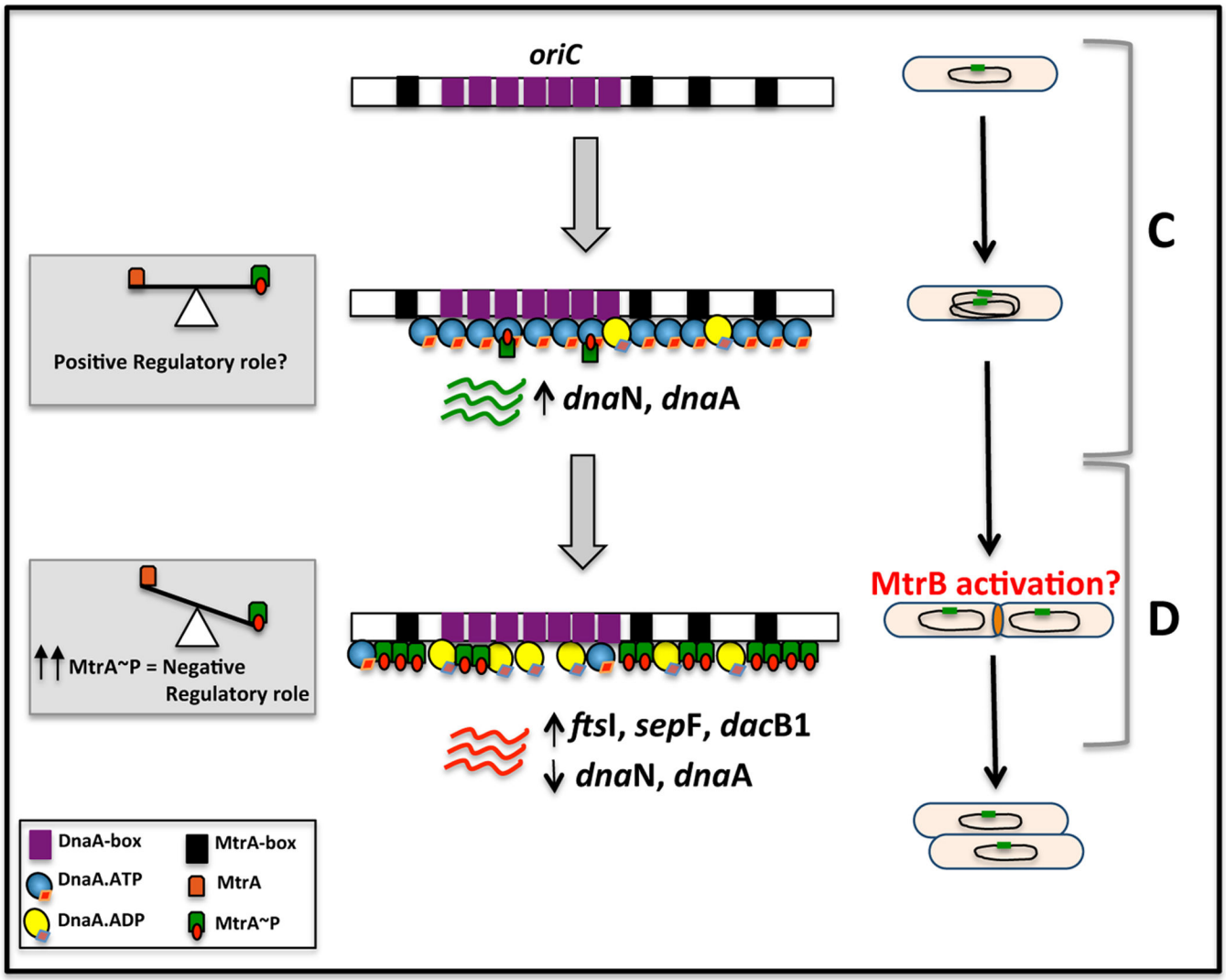

Fig. 10.

Cartoon showing the MtrA-mediated regulatory effects on *oriC* replication and cell cycle progression: *M. tuberculosis oriC* with MtrA-boxes (black) and DnaA-boxes (magenta) is shown to the left and cell cycle progression with C and D periods are shown to the right. Note the non-overlapping arrangement of the DnaA- and MtrA-binding sites in *ori*C implies that the binding of MtrA~P and DnaA to their respective binding sites proceed independently. MtrA activity, i.e. the ratio of MtrA to MtrA~P, is shown in equilibrium in the C period whereas shown altered with increased MtrA~P in the D period. MtrB sensor kinase activation is proposed occur in the D period, thereby trigger elevated MtrA~P. Accordingly, the transcriptions of *dnaA* and *dnaN* are shown elevated in the C period and reduced in the D period. Also, increased transcription of *ftsI*, *dacB1*, *sepF* are shown in the D period. Because the ATPase activity of DnaA is required for its rapid oligomerization on *oriC* (Madiraju et al., 2006) and *oriC* unwinding (Kumar et al., 2009), binding of both DnaA.ATP and DnaA.ADP forms to *oriC* in the C period are shown. Although significant *oriC* enrichment by MtrA does not occur in the C period, MtrA~P may also associate with

DnaA. MtrA access to *oriC* in the D period is either direct and or could be aided by DnaA. A consequence of the negative regulatory role of MtrA~P (marked in the D period) would be the prevention of hyper-replication and promotion of regulated cell cycle progression. Reduction in MtrA~P pools at the end of D period could release MtrA from *oriC*; but MtrA~P may remain associate with DnaA to promote *orisome* assembly and another cycle of DnaA-mediated *ori*C replication. This positive regulatory role of MtrA~P could also involve interactions with other components of replisome machinery. However, the molecular details as to how these events occur are unknown. Nonetheless, the presumptive positive regulatory role is marked in the C period.